Sede Amministrativa: Università degli Studi di Padova

Dipartimento di Istologia, Microbiologia e Biotecnologie Mediche

Sezione di Istologia ed Embriologia

SCUOLA DI DOTTORATO DI RICERCA IN: BIOMEDICINA

CICLO: XXIV

Role of TGF-βs growth factors in development of aortic aneurysms. Study in a mouse model of Marfan syndrome.

Direttore della Scuola: Ch.mo Prof. Giorgio Palù

Supervisore: Ch.mo Prof. Giorgio M. Bressan

Dottorando: Francesco Da Ros

THESIS CONTENTS

ABBREVIATIONS

AAA: abdominal aortic aneurysm
ALK: activin receptor-like kinase
BMP: Bone Morphogenic Protein
BMPr: Bone Morphogenic Protein receptor
bp: base pair
BSA: bovine serum albumin
C-terminal: carboxyl terminal
ca: constitutively active
Ctgf: connective tissue growth factor
DMEM: Dulbecco's modified Eagle medium
DTT:1,4-Dithiothreitol
ECM: extracellular matrix
ECs: endothelial cells
EDTA: ethylenediaminetetraacetic acid
EL: elastic lamellae
Fbn1: Fibrillin-1
Fbln4:Fibulin-4
FBS: fetal bovine serum
H&E: hematoxilin and eosin staining
H2BGFP: histone conjugated green fluorescent protein
HcRed: *Heteractis crispa* red fluorescent protein
HRP: horseradish peroxidase
IEL: internal elastic lamellae
Id: inhibitor of DNA binding
LAP: latency associated peptide
LLC: large latent complex
LTBP: latent TGFβ-binding protein
MFS: Marfan syndrome
NP40: Nonidet P40
PAI-1: plasminogen activator inhibitor-1
PBS: phosphate-buffered saline
PCR: polymerase chain reaction
ROS: reactive oxygen species
rtTA: reverse tetracycline transactivator
SLC: small latent complex
Smmhc: smooth muscle myosin heavy chain
VSMCs: vascular smooth muscle cells
TAA: thoracic aortic aneurysm
TBS: Tris buffered saline
TGF-β: transforming growth factor beta
TGFβr: transforming growth factor beta receptor
TRE: tetracycline responsive elements
TUNEL: Terminal deoxynucleotidyl transferase-mediated dUTP nick and labelling

ABSTRACT

This study is a first part of a larger project that concerns analysis of vascular anomalies, in particular aortic aneurysm, in Marfan syndrome (MFS). MFS is a systemic disorder that principally interests skeletal, ocular and vascular systems. Although it is clearly defined that *Fbn1* mutations are the principal cause of syndrome manifestation, the pathogenic mechanism of phenotypic alteration, like aortic aneurysm, remains unclear. Since Fibrillin-1 functions as storage of growth factors, the deregulation of TGF-β signaling has been suggested as starting event in manifestation and progression of aortic aneurysm. In accordance with this hypothesis, the study of Marfan mice models, as *Fbn1*$^{+/C1039G}$ model, having a point mutation corresponding to that found in human subjects, revealed an increase of P-Smad2/3 and of TGF-β target genes expression in aortic aneurysm. However, other findings suggested the involvement of other signaling pathways (Angiotensin II, MAPK), while a role for BMP has never been considered, even if BMP binds Fibrillin-1 and is involved in skeletal alterations of Marfan syndrome.

In this work we analyzed activation levels of TGF-β/BMP signaling in *Fbn1*$^{+/C1039G}$ mice, at different ages and in both aortic arch and descending aorta. *Fbn1* mutants showed increase of both signaling at 2 and 4 months, but not at 7 months when aneurysm is observed. Analysis has also highlighted lack of correlation between expression of TGF-β target genes, PAI-1 and Ctgf, and P-Smad2/3 levels in aortic arch in 7-month-old mice suggesting implication of other signaling pathways. Analysis of BMP target genes expression has shown a correspondence between Id2 and phosphorylation levels of Smad1/5/8; instead Id3 was still increased at 7 months, suggesting that its expression at this age may be regulated by other factors.

One main effort of the study was the generation of a transgenic inducible expression system, based on Tet-On technology, to modulate TGF-β/BMP signaling in smooth muscle cells of aorta. We generated transgenic mouse lines for reverse tetracycline transactivator (rtTA), controlled by *Smmhc* promoter, and for responsive constructs (caALK5, caAlk3, Smad7, Smad6, Noggin) under TRE-

CMVmin promoter. RT-PCR analysis *in vitro* in VSMCs and *in vivo* in aorta of double transgenic mice showed appropriate function of the inducible system and partial correlation between modulated signaling and target gene expression.

To address the role of combined TGF-β/BMP signaling in aneurysm development *Smad4* was inactivated in smooth muscle cells of adult wild-type and *Fbn1* mutant mice using conditional inducible gene knockout. In wild-type mice, inhibition of both signaling pathways caused the appearance of vessel wall damage, aortic arch dilatation and death for dissection within 6 months from gene inactivation induction. *Smad4* knockout in smooth muscle cells of *Fbn1* mutant mice determined worsening of thoracic aortic aneurysm, with increase of aortic root dilatation and aortic wall damage. Besides, $Fbn1^{+/C1039G}$ mice with *Smad4* inactivation, developed also abdominal aortic aneurysm, a finding that was never observed in $Fbn1^{+/C1039G}$ mice. Increase of structural damage in *Fbn1* and *Smad4* mutants caused early death for dissection, rarely documented in $Fbn1^{+/C1039G}$ mice.

These observations suggest a protective role of TGF-β/BMP activity in the formation and the progression of aortic aneurysms. These results will be expanded and supplemented by a detailed molecular analysis of additional signaling pathways that are deemed to play a role in Marfan syndrome.

RIASSUNTO

Lo studio qui presentato, si propone di porre le basi per un progetto che interessa l'analisi delle anomalie vascolari, in particolare aneurisma aortico, nella sindrome di Marfan, malattia sistemica che colpisce principalmente i sistemi scheletrico, oculare e vascolare. Anche se è ormai dimostrato che anomalie a carico del gene *Fbn1*, che codifica per una proteina delle fibre elastiche, la Fibrillina-1, sono la causa principale dell'insorgenza della malattia, risulta ancora poco chiara la patogenesi delle alterazioni fenotipiche, in particolare dell'aneurisma aortico. Considerando la funzione della Fibrillina-1 come deposito di fattori di crescita, l'ipotesi attualmente più accreditata, suggerisce che ci sia una alterata regolazione del segnale di TGF-β alla base della manifestazione e progressione dell'aneurisma aortico. Concordemente a questa ipotesi, l'analisi di modelli animali, come i topi *Fbn1*$^{+/C1039G}$, che portano una mutazione puntiforme di una aminoacido frequentemente mutato nella sindrome di Marfan, ha riscontrato un incremento di P-Smad2/3 e di espressione di geni bersaglio di TGF-β a livello dell'aneurisma. Tuttavia, i dati hanno suggerito la possibile implicazione di altre vie di segnale (Angiotensina II, MAPK), mentre non è stato considerato il ruolo di BMP, un fattore di crescita che lega direttamente la Fibrillina-1 e di cui è stato prospettato un ruolo nelle alterazioni scheletriche della sindrome.

In questo studio abbiamo inizialmente analizzato i livelli di attivazione delle vie del TGF-β e BMP a diverse età a livello dell'arco aortico e nel tratto discendente dell'aorta in topi *Fbn1*$^{+/C1039G}$. Nei *Fbn1* mutanti, i dati mostrano un incremento del segnale di entrambe le vie a 2 e 4 mesi, ma non a 7 mesi, quando invece l'aneurisma è presente. L'analisi ha poi evidenziato una mancata correlazione tra i livelli di espressione di PAI-1 e Ctgf, geni bersaglio per TGF-β, e P-Smad2/3 a livello dell'arco aortico a 7 mesi, suggerendo l'implicazione di altre vie di segnale. Per quanto riguarda l'espressione dei geni bersaglio di BMP, è stata osservata corrispondenza tra l'espressione di Id2 e i livelli di P-Smad1/5/8; Id3 invece, rimane aumentato nei mutanti anche a 7 mesi, evocando, anche in questo caso, la possibilità dell'intervento di altri fattori. Lo studio ha

inoltre previsto la generazione di un sistema di espressione inducibile, basato sulla tecnologia del sistema Tet-On, sensibile alla doxiciclina, per la modulazione delle vie di TGF-β/BMP nella cellule muscolari lisce di aorta (CMLV). Sono state generate linee transgeniche per il transattivatore (rtTA), controllato dal promotore del gene *Smmhc*, e per i geni bersaglio (caALK5, caAlk3, Smad7, Smad6, Noggin) controllati dal promotore inducibile TRE-CMVmin. Le analisi di RT-PCR *in vitro* in CMLV ed *in vivo* in aorta di topi doppi transgenici, hanno evidenziato il corretto funzionamento del sistema inducibile e la parziale correlazione tra via di segnale modulata ed espressione dei geni bersaglio.

Contemporaneamente utilizzando la linea transgenica *Smmhc*-CreER^{T2} è stata indotta l'inattivazione del gene *Smad4* in topi adulti mutanti e non per *Fbn1*. L'inibizione di entrambe le vie di segnale comporta già in topi non mutanti, la comparsa di danno di parete, dilatazione a livello dell'arco aortico e morte per dissezione aortica entro 6 mesi dall'inattivazione del gene. Inoltre la mancanza di *Smad4* nelle CMLV in topi *Fbn1*$^{+/C1039G}$ causa un peggioramento dell'aneurisma toracico, caratterizzato da incremento della dilatazione aortica e del danno parietale. In aggiunta nei topi *Fbn1*$^{+/C1039G}$, *knockout* per *Smad4*, si sviluppa anche un aneurisma addominale, normalmente mai osservato nei modelli Marfan. L'incremento del danno strutturale nei topi mutanti per *Fbn1* e *Smad4* porta a morte precoce per rottura dell'aneurisma, un evento che si verifica molto raramente nei topi con la sola mutazione di *Fbn1*.

Queste prime osservazioni, che andranno ampliate e affiancate da uno studio molecolare delle vie di segnale sopra menzionate, suggeriscono un effetto protettivo di TGF-β/BMP nella comparsa e progressione di aneurismi aortici. Questa considerazione trova conferma nei dati relativi ad incremento di dissezione ed aneurisma aortico, in seguito ad inibizione di TGF-β, in modelli animali diversi da quello qui analizzato.

INTRODUCTION

The elastic extracellular matrix

The extracellular matrix (ECM) is a tridimensional network of macromolecules that confers strength and stability to tissues and organs and controls cell behavior through interactions with specific cell surface receptors. The synthesis, deposition and degradation of the numerous components of the matrix are regulated by a several growth factors. Conversely, the activity of a variety of growth factors is regulated by some components of the ECM and of the elastic matrix in particular (Vehviläinen et al., 2009; F. Ramirez and D.B. Rifkin, 2009).

This study deals with blood vessels, whose ECM is a scaffold that endows the vessel with the capacity to resist tensile stress and to maintain the shape of the vessel through elastic recoil. In large elastic conducting vessels, such as aorta, collagens and elastic fibers are the major components of ECM.

Elastic fibers are the component of the ECM responsible for resilience and elastic recoil and are especially abundant in lung and skin in addition to elastic arteries. Biochemical and ultra-structural analyses have demonstrated that elastic fibers are formed by two morphologically distinct components (Greenlee et al., 1966): a central amorphous nucleus consisting of Elastin, a fibrous protein responsible for the elastic properties of the fiber, and a surrounding coat of microfibrils, composed primarily by Fibrillin-1 and -2 (Sakai et al., 1986, Zhang et al., 1994). Both components carry out regulatory functions. Fibrillin-1 and -2 are important in the control of availability of growth factors of the TGF-β family (specifically TGF-βs and some Bone Morphogenic Proteins, BMPs). The regulatory function of Elastin is highlighted by the intriguing phenotype observed in null mice: pups die soon after birth due to subendothelial proliferation of smooth muscle cells which reduces considerably the lumen of blood vessels (Li et al., 1998). In fact, Elastin inhibits cell proliferation via a non-integrin, heterotrimeric G-protein-coupled pathway and the observed alterations are due to lack of this inhibition (Karnik et al., 2003). Interestingly, Elastin has also a role in determining the structure of blood vessels: heterozygous mutant mice have an

increased number of elastic lamellae (Li et al., 1998), and loss of function of one *ELASTIN* allele in humans induces sopravalvular aortic stenosis, in which narrowing of the vessel wall is the consequence of the increased thickness of the media determined by a higher number of elastic lamellae (Curran et al., 1993). Although the molecular details of how these modifications are brought about are not known, they indicate that Elastin has important effects on the behavior of vascular cells. Interestingly, *Elastin* null heterozygous mice develop arterial systemic hypertension (Faury et al., 2003). This trait is also observed in mice deficient of *Fibulin-5* (Yanagisawa et al., 2002) and *Emilin1* (Zacchigna et al., 2006), two other proteins of elastic fibers associated with the amorphous core. All these data strongly suggest that elastic fibers are key modulators of vascular cells function and that, through action on the cells, they regulate structural remodeling of blood vessels and important physiological parameters such as arterial blood pressure.

Maturation and signaling of TGF-β and BMP

There are three isoforms of TGF-β, TGF-β1, 2 and 3, coded by three different genes and all expressed as a precursor, called proTGF-β. The propeptide is cleaved in the secretory pathway by furine enzymes, but it remains non-covalently linked to the mature TGF-β with the name of LAP (Latency Associated Protein), forming the Small Latent Complex (SLC). The SLC is associated with one of the LTBPs (Latent TGF-β Binding Protein) isoforms, composing the LLC (Large Latent Complex) that is finally secreted. In the extracellular space, this latent form of TGF-β binds to the proteins of the ECM Fibrillin-1 and Fibronectin (Dabovic et al., 2002; Mazzieri et al., 2005). In the LLC, mature TGF-β is inactive and needs the action of different kinds of activators to become able to bind the specific receptors on cellular membrane. Activation requires dissociation of the SLC and is mediated by trombospondin1, integrins, ROS (Reactive Oxygen Species) or proteolitic activity (Annes et al., 2003).

Two different types of cell surface receptors are required for TGF-β signaling, the constitutively active TGFβrII and the three TGFβrI , Alk5, Alk4 and Alk1. After the binding of TGF-β to TGFβrII, the TGFβrI is recruited and activated

after phosphorylation mediated by serine/threonine kinase activity of TGFβrII. The heterocomplex TGFβrII/TGFβrI phosphorylates and activates specific transcription factors called receptor-regulated (R) Smad proteins, Smad2/3. The active Smads (P-Smad2/3) bind a Co-mediator (Co-Smad) (Smad4) and translocate to the nucleus to regulate target genes expression. (Agrotis et al., 2005).

Bone Morphogenic Proteins (BMPs) also belong to the TGF-β family and are expressed in different isoforms (1-20). BMPs are secreted directly as active factors, as omo or heterodimers. As for TGF-β1, 2 and 3, also BMPs have two different types of receptors. Three types of BMPrII, BMPrIIa, ActRIIa and ActRIIb, and three type of BMP receptor I, ActRIa o Alk2, BMPrIa or Alk3, BMPrIb or Alk6, are known. The regulation of the signaling of BMP is similar to the one described for TGF-β, but different R-Smads, Smad1-5-8, are involved (Miyazono et al. 2005; Sieber et al., 2009).

The signaling is also negatively regulated by inhibitory (I-Smads), Smad7 for TGF-β and Smad6 for BMP (Fig. 1.1).

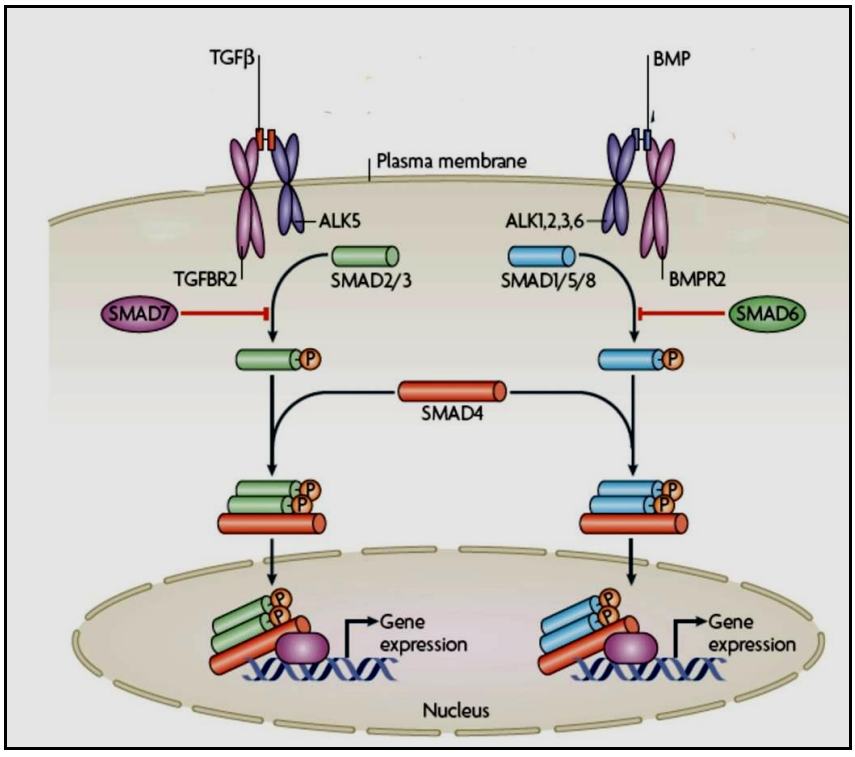

Figure 1.1. Scheme of TGF-β and BMP signaling. *(P. ten Dijke and H. M. Arthur 2007)*

The Fibrillins

The Fibrillins (Fibrillin-1, -2 and -3) are large cysteine-rich proteins of elastic extracellular matrix that self-assemble into sovramolecular structures called elastic fiber microfibrils. The important role of Fibrillins derives from their structural features, that allows the binding and control of several different ECM proteins (Elastin, Fibulin-4 and -5, proteoglicans, lysyl oxidase, Fibronectin, MAGPs), but also integrins and growth factors (F. Ramirez and L. Y. Sakai, 2009). One of the major important Fibrillins role is the control of the bioavailability of BMPs and TGF-βs, a function that they share with Emilin1, MAGP-1 and Fibulin4, (F. Ramirez and D.B. Rifkin, 2009). In particular, Fibrillin-1 binds in different ways the two growth factors. The latent form of the TGF-β is bound to Latent TGF-β binding protein (LTBP1 and 4). The LTBPs are structurally related to Fibrillins and participate in TGF-β regulation, partly by targeting TGF-β complexes to the ECM. Deeper knowledge of the structure of LTBPs and TGF-β1 revealed that exist a force-dependent mechanism for growth factor activation that depends on αV integrins (Shi et al., 2011).

Differently, not all BMP isoforms have a latent state during maturation (Sieber et al., 2009) and it is known that the prodomain of all BMP isoforms binds directly to Fibrillin-1, although it is not completely clear how the activation process is regulated (Sengle et al., 2008; F. Ramirez and L.Y. Sakai, 2009).

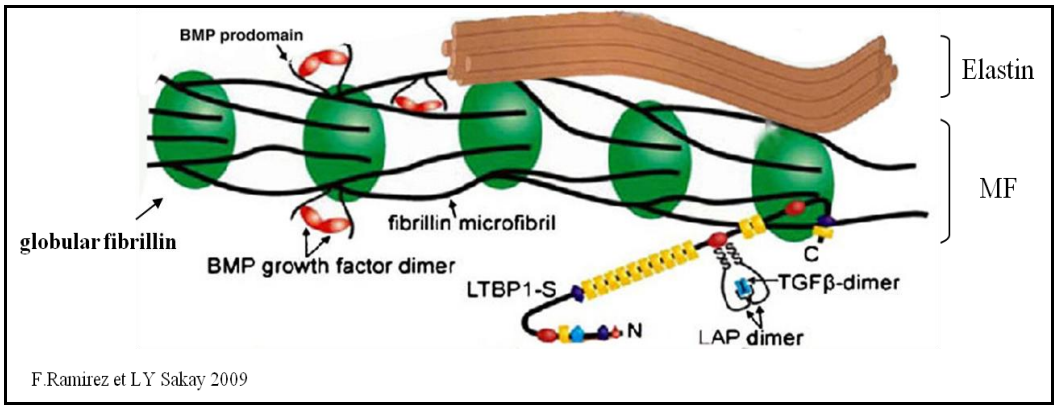

Figure 1.2. Schematic representation of elastic fibers. Fibrillins bind directly BMPs and indirectly TGF-βs, through LTBP proteins. MF: microfibrillae. (F. Ramirez and L.Y. Sakay, 2009)

Mice models of Marfan syndrome and TGF-β activation

Marfan syndrome is a systemic disorder of connective tissue affecting mainly vascular, skeletal and ocular systems and caused by mutations in the *Fbn1* gene, encoding Fibrillin-1. The incidence of classic Marfan syndrome is about 2-3 per 10000 individuals. The syndrome affects skeletal, ocular and vascular system, with effects also in other tissues as lung. The skeletal development is altered and Marfan patients present overgrowth of long bones, aracnodactlyly, and scoliosis and they show ocular dislocation (D.P. Judge and H.C. Dietz, 2005). Manifestations of Marfan syndrome in the cardiovascular system are conveniently divided into those affecting the heart and those affecting the vasculature. Within the heart, the atrioventricular valves are mostly affected, with thickening of the valves. However the major life-threatening manifestations of Marfan syndrome are aortic aneurysm and dissection.

Aortic aneurysm (AA) usually increases predisposition to aortic dissection. Two predominant types of aneurysm are recognized, abdominal aortic aneurysm (AAA) and thoracic aortic aneurysm (TAA). The first is characterized by invasion of inflammatory cells into the aortic wall, with consequent matrix disruption and VSMCs depletion. Features of TAA are instead destructive matrix remodeling with elastic fibers fragmentation, VSMCs proliferation but low inflammatory component. Familial TAA are subdivided in syndromic, as in Marfan syndrome, or non syndromic presentation.

Actually there are different mouse models for Marfan syndrome. Mice lacking or under expressing Fibrillin-1 die at postnatal days 10–14 (P10–P14) (mgN/mgN mice) and at 2–6 months of age (mgR/mgR mice), respectively. Although these models present typical manifestations of Marfan syndrome (F. Ramirez and L.Y. Sakai, 2009), they are not useful for long term analysis of pathology progression. Indeed, actually, the most studied model is a heterozygous mouse carrying a missense mutation of *Fbn1* (Cys 1039 > Gly), corresponding to one of the of *FBN1* mutation detected in Marfan human subjects (C1039Y) (Shrijver et al., 1999). This mutation determines a change in the normal deposition and organization of Fibrillin-1 in elastic matrix. Mice homozygous for the mutation die in perinatal period, while heterozygous mice show a progressive

aortic root dilatation, with thickening of the aortic media due to deposition of amorphous matrix and fragmentation and disarray of elastic lamellae. Moreover, the *Fbn1*$^{+/C1039G}$ model exhibits skeletal alterations that mimic those found in Marfan subject, like kyphosis and overgrowth of the ribs (Judge et al., 2004; Habashi et al., 2006).

Mouse models for MFS have been very useful in revealing that mutations in the Fibrillin-1 gene promote promiscuous activation of latent TGF-β, as demonstrated by increased phosphorylation of Smad2/3 and expression of target genes as PAI-1 and Collagen1 in the wall of aorta of Fibrillin-1 mutants (Habashi et al., 2006; Neptune et al., 2003; F. Ramirez and D.B. Rifkin, 2009). Moreover the blockade of TGF-β signaling with neutralizing antibodies against all TGF-β isoforms in 7 weeks old *Fbn1*$^{+/C1039G}$ mice rescued the vascular phenotype, as evidenced by a normal morphology of elastic lamellae and thickness in the aortic media.

Other signaling pathways with potential impact on Marfan phenotype

Intriguingly, phenotype rescue in Marfan mice was also achieved with inhibition of Angiotensin II signaling, which is known to modulate TGF-β signaling (Cohn et al., 2007), through blockade of AT-1 receptor with Losartan (Habashi et al., 2006). However, the inhibition of Angiotensin II with Losartan allows also the inhibition of matrix metalloproteases (MMP) 2 and 9, whose expression and activity are augmented in *Fbn1*$^{+/C1039G}$ mice, and that may be responsible for the disarray observed in aortic media of mouse models of Marfan syndrome (Chung et al., 2007). Thus, it is not clear if and by which mechanism, Angiotensin II could be implicated in the appearance of aortic aneurysm, particularly of those found in Marfan syndrome. Angiotensin II might act enhancing TGF-β signaling, by positive feedback. Moreover, the role of physiological modifications of aorta in the development of aneurysms in Marfan mouse models has not been established. Indeed in Marfan model mice was found a reduced contraction of the mesenteric vessel to phenylephrine and potassium, associated with decrease of Ca^{2+} wave frequency of VSMCs and an age-dependent increase of stiffness of aortic wall (Syyong et al., 2009; Syyong et al., 2011). This altered response seems to be

due to a reduction of NO synthesis by endothelial cells (ECs). A final comment is also worth on studies on ECs function in *Fbn1* mutant mice. Even if the treatment with Losartan improves aortic dilatation, there is no change in the impaired production of nitric oxide (NO) by ECs in mutants *Fbn1*$^{+/C1039G}$ (Yang et al., 2009). A recent paper shows the importance of the other receptor for Angiotensin II, AT-2, for the survival of *Fbn1* mutant mice: the deletion of AT-2 expression in *Fbn1*$^{+/C1039G}$ mice worsened the aortic phenotype and increased mortality for dissection (Habashi et al., 2006; Habashi et al., 2011). This data confirms that Angiotensin II is an important regulator of functional and morphological properties of aorta in mouse models of Marfan syndrome, in addition to the well established role in the development of other type of aneurysm, such as those observed in Fibulin-4 deficient mice and abdominal aortic aneurysms.

Fibulin-4 is a secreted glycoprotein of the ECM, involved in the formation of elastic fibers (Argraves et al., 2003). Mice with absent or reduced expression of *Fbln4* (e.g. *Fbln4*-deficient mice or hypomorphic *Fbln4* R/R mice, respectively) show progressive severe thoracic aortic aneurysm (TAA), high mortality, elastic fibers fragmentations and losses of smooth muscle cells. The aortic contractile capacity is diminished, due to a deregulation of contractile genes. Increased phosphorylation of Smad2 in aortic wall and augmented tissue level of Angiotensin II have been observed in these mutants. Prenatal treatment of *Fbln4* R/R mice with Losartan prevented elastic fibers fragmentation, instead postnatal blockade of Angiotensin II only improved lifespan of mice without affecting wall structure (Moltzer et al., 2011).

Recent studies in Vascular Smooth Muscle Cells (VSMCs) isolated from null (mgN/mgN), underexpressing (mgR/mgR) or mutant (*Fbn1*$^{+/C1039G}$) mice show an activation of P-Smad2/3 in all mouse models, indicating that the alterations in the aortic wall may be cell-autonomous and directly linked to the muscular component of the vessel. However, the analyses in mgN/mgN mice, which exhibit the highest P-Smad2/3 levels, show that enhancement of TGF-β signaling is secondary to activation of p-38 MAPK. Consistent with these cell culture data, *in vivo* analyses documented that phospho-p38 MAPK accumulates earlier than phospho-Smad2 in the aortic wall of mgN/mgN mice and that systemic inhibition of phospho-p38 MAPK activity lowers the levels of P-Smad2 in

this tissue (Carta et al., 2009). An important work by Dietz and collaborators, describing the reversal of the phenotype by pharmacological inhibition of ERK1/2 activity, also highlight the role of MAPKs in the pathogenesis of Marfan syndrome (Holm et al., 2011). The authors conclude that aneurysm development is due to simultaneous increase of TGF-β canonical and the non-canonical signaling pathways, the former being transduced through Smads phosphorylation, the latter through activation of the MAPK ERK1/2 (Fig. 1.3).

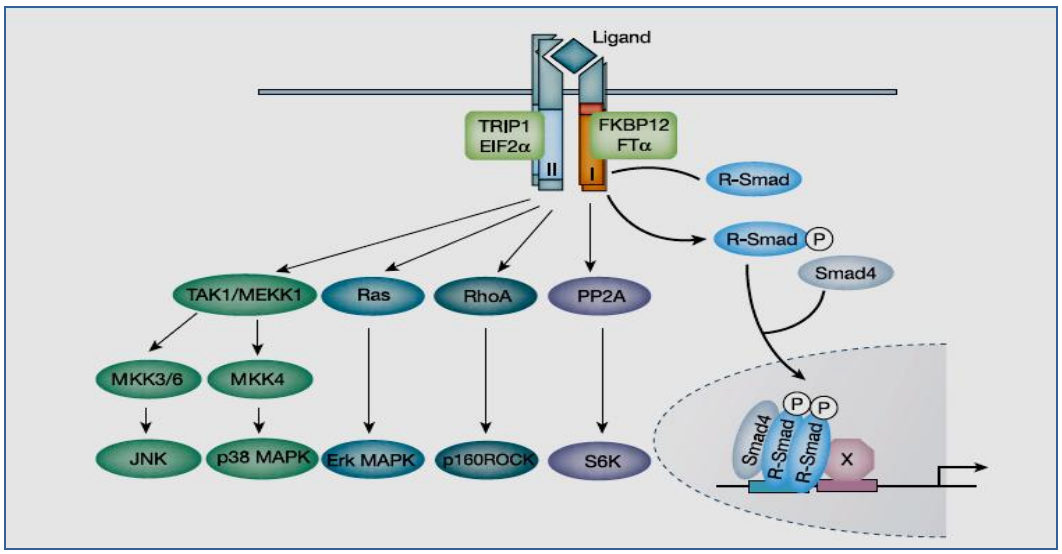

Figure 1.3. Smad-dependent and Smad-indipendent pathways in TGF-β family signaling. *(Derynck et Zhang 2003)*

Pathogenetic hypotheses of aneurysm formation in Marfan syndrome

About the pathogenesis of TAA in Marfan syndrome, initial attention was focused on elastic fibers alteration and disorganization as a principal factor responsible for aneurysm progression. However, not all studies in mouse models deficient for protein involved in elastic fibers organization show thoracic aortic aneurysm as Fibrillin-1 and Fibulin-4 deficient mice. For example TAA is not present in Fibulin-5 or Elastin deficient animals (M.E. Lindsay and H.C Dietz, 2011). In addition, the analysis of a mouse model that is deficient for Fibrillin-1, evidences lung abnormalities even in the immediate postnatal period. This suggests that early development perturbations, due to Fibrillin-1 alterations,

predispose to tissues modifications and disease manifestations (Neptune et al., 2003).

As mentioned above, Dietz and colleagues found in different mouse models for Marfan syndrome, an increased in TGF-β signaling, as indicated by circulating TGF-β, P-Smad2 and PAI-1 expression levels (Neptune et al., 2003; Matt et al., 2009; Habashi et al., 2006; Holm et al., 2011). Moreover, rescue of vessel phenotype is obtained with inhibition of TGF-β signaling by blocking with specific Abs or treatment with Losartan (Habashi et al., 2006).

Studies in human also point to TGF-β pathway as a major player in aneurysm development. The results, however, do not allow the straightforward conclusion that TGF-β favors aneurysm formation. Thus, in TGFβrII, missense and abnormal splicing mutations have been associated with Marfan syndrome type 2; surprisingly, all mutations produced loss of function of the TGF-β type II receptor (Mizuguchi et al., 2004). In a study on patients affected by Loeys-Dietz syndrome, a complex syndrome including marked tortuosity of aorta and aortic root and subclavian aneurysms, it was found that a subgroup of patients presented mutations in TGFβrI or TGFβrII (Loeys et al., 2006). It was noted that, although mutations crippled receptors function, examined tissues exhibited features that can be ascribed to increased TGF-β signaling. More recently, a syndromic form of aortic aneurysms and dissections have been linked to mutations of SMAD3 (van de Laar et al., 2011). Again, although mutations inactivated SMAD3 function, increased aortic expression of several key players in the TGF-β pathway was detected. To explain these contradictory results it has been postulated that deficient receptor (or SMAD3) function may stimulate compensatory TGF-β production, resulting in enhanced activation of the canonical and non-canonical TGF-β pathways, despite the inactivating character of the mutation (M.E. Lindsay and H.C. Dietz, 2011).

Results even more difficult to reconcile with the tenet that increased TGF-β signaling is instrumental for aneurysm development in Marfan syndrome, what found in the *Fbn1*$^{+/C1039G}$ mouse by Holm et al. (2011). The authors showed, surprisingly, that the inactivation of one *Smad4* allele in mutant *Fbn1*$^{+/C1039G}$ mice caused worsening, and not an improvement, of aortic aneurysm progression, with augmented damaged area (aortic root and ascending aorta, the latter being rarely

involved in TAA) and increased death for dissection starting after few weeks from birth. To explain this paradoxical effect the authors noted that, despite reduction of *Smad4* dosage, canonical TGF-β signaling, as monitored by P-Smad2/3 levels, was increased and that Jun N-terminal kinase (JNK) activity was enhanced, likely through non-canonical TGF-β signaling (Fig. 1.3). Supporting this suggestion, it was found that pharmacological inhibition of JNK *in vivo* in *Fbn1*$^{+/C1039G}$ mice delays aneurysm progression and improves aortic wall structure (Holm et al., 2011).

Another important point to consider is that, at today, there has been no analysis on the effect of genetic inhibition of TGF-β in Marfan models. The only direct evidence of implications of TGF-β in aortic aneurysm progression derives from treatment with antibody anti-TGF-β of *Fbn1*$^{+/C1039G}$ mice, that can probably interfere with other pathways (BMP) which are not considered in the study (Habashi et al., 2006).

In summary, it can be noted that the mechanisms of pathogenesis of aneurysm, as well as of other symptoms, in Marfan syndrome is still an unsettled issue. Although TGF-β signaling seems to be involved, it is not clear whether it has an instrumental role in the lesion or it is a compensatory mechanism reducing the severity of aneurysm progression.

Aims of the study

As described before, mice with a heterozygous mutation in *Fbn1* allele (*Fbn1*$^{+/C1039G}$) are important models for Marfan syndrome. The altered production of Fibrillin-1 determines the appearance of progressive aortic aneurysm, particular evident in the root and ascending tract of the vessel, with disorganization and alteration of the media, rupture of elastic lamellae and deposition of amorphous extracellular matrix. Recent studies *in vitro* has revealed that some molecular alterations observed in the aorta of MFS mice are maintained in the VSMCs, as activation of TGF-β signaling and the kinase p38 (Carta et al., 2009).

Starting from the data discussed before, in this study we wanted to investigate the real role of TGF-β/BMP in the appearance of the aortic aneurism

observed in MFS mice. Initially we wanted to analyze the activation levels of these two growth factors in different aortic segments, detecting the amount of P-Smads and target gene expression levels. To deepen the understanding of the effects of TGF-β/BMP pathway in aneurysm manifestation and progression, we used two different approaches so as to modulate these signaling in VSMCs.

The first approach was the generation of transgenic mice in a doxycycline inducible expression system, where the reverse tetracycline transactivator (rtTA) of the Tet-On system drive by the specific smooth muscle promoter *Smmhc* (smooth muscle myosin heavy chain), to control expression of different genes involved in TGF-β/BMP signaling: constitutively active receptor for TGF-β or BMP, or inhibitor as I-Smad (Smad 7 and 6 respectively) and Noggin for BMP. At the same time we used a mouse transgenic line expressing the inducible $CreER^{T2}$ recombinase under the same promoter. The action of Cre-recombinase after induction with tamoxifen was used to induce the deletion of a *Smad4* floxed allele and to evaluate the effects of inhibition of both TGF-β and BMP signaling in wt background or *Fbn1* mutant mice in vessel phenotype. The data obtained will be useful to discuss whether the TGF-β may have a protective role in the appearance of aortic aneurysm. Apart from data shown by Holm and colleagues, another work raises doubts about this point. Indeed Wang and colleagues discover that systemic neutralization of TGF-β in normocholesterol C57BL/6 mice breaks the resistance to Angiotensin-II aortic aneurysm formation, characterized by smooth muscle cell death, elastin degradation and enhanced vascular inflammation, with increased number of macrophages and lymphocytes in the media (Wang et al., 2010).

MATERIALS AND METHODS

Mouse strains and treatment

Procedures involving animals and their care were conducted according to institutional guidelines in compliance with national laws. Smad4$^{f/f}$ mice were a gift of professor S. Piccolo. The mouse model for Marfan Syndrome (*Fbn1*$^{+/C1039G}$) was kindly given by Dietz HC laboratory.

Doxycycline treatment of transgenic mice carrying the rtTA transgene and the corresponding controls was performed via drinking water at the concentration of 1mg/ml or 10mg/ml, using dark bottles to protect doxycycline from light-degradation. The solution was changed every two days. Tamoxifen was administered using commercially available chows (Tam400, 400mg/kg; Harlan) for 10 days.

Generation of DNA constructs

Driver construct: Smmhc-rtTA

The BAC clone RP-156B9 (CHORI) of 160 Kb spanning smooth muscle myosin heavy chain gene and chloramphenicol resistance gene was amplified in SW102 bacteria strain and modified with recombineering protocol in order to insert rtTA cDNA under *Smmhc* promoter. rtTA cDNA was slightly modified by adding at the 5' and the 3' end 500bp of the homologous region flanking ATG triplet of *Smmhc* gene. The two genomic regions were amplified from the BAC clone with the following primers: for the 5' end Forward primer: ACTAGT-AGATCCGGGATCATCTGATGG and Reverse primer: CCGCGG-GATGTCTGG TGGTCCCCTG; for the 3' end Forward primer: AAGCTT-GCGCAGAAA GGGCAGCTC and Reverse primer: AAGCTT-GCCCAGGCTAGCCTTGAAC. The PCR products were inserted in pTetOn respectively at the 5' end of rtTA between SpeI and SacII (underlined primer sequence) and at 3'of rtTA in HindIII in pTetON-5'arm obtaining the construct 500-rtTA-500. The SW102 bacterial

strain containing the BAC clone carries a lambda system for homologous recombination, that must be activated at 42°C for 15 minutes. After activation, 500-rtTA-500 cDNA was electroporated in SW102 (1,75 V; 200 Ohm; 25 µF; Pulse Control, Bio Rad), then seeded on chloramphenicol containing bacterial plates. PCR on rtTA was made as first screen to detect positive colonies (primer table 2.2). PCR positive samples were then tested with restriction enzyme digestion that discriminates between wild-type and modified BAC. DNA of modified BAC, *Smmhc*-rtTA, was purified with Maxy prep kit (Qiagen), linearized and used for pronuclear microinjection in fertilized oocytes at the concentration of 1,5 ng/µl in injection buffer (Tris-HCl 10 mM, EDTA 0.1 mM pH 8). Transgenic mouse lines and embryos were produced from B6D2F1 females mated with B6D2F1 males (Charles River Italia) using standard procedures (Nagy et al., 2003). DNA was microinjected into pronuclei of one-cell embryos and the surviving embryos were implanted into CD1 pseudopregnant foster mothers.

Responsive constructs

pKS-STOP-TRE-CMV-MCS (pKS-STOP-TC)

Tetracycline Responsive Element (TRE)-CMVminimal promoter was amplified from pTRE-Tight (Clontech) to insert the restriction enzyme sites for EcoRV-BglII at 5' end and for HindIII at 3' end (Forward: GATATC-ga-AGATCT-tc-CTTTCGTCTTCAATCGAGTTTAC, the Yellow highlighted A was inserted instead of a C to delete a XhoI site; Reverse: AAGCTT-CAGGCGATCTGA CGTTC). The EcoRV-BglII-TRE-CMV-HindIII fragment was cloned in Bluescript pKS EcoRV-HindIII (pKS-TRE-CMV). The BamHI-STOP-BamHI cassette of 1383bp, purified from the plasmid pBS302 (Addgene), was then insert at the BglII site of pKS-TRE-CMV, obtaining pKS-STOP-TRE-CMV plasmid.

A multiple cloning site (MCS: HindIII-SwaI-BamhI-XbaI-XhoI-XmaI-NdeI-SalI) was cloned between the HindIII and SalI sites in the pKS-STOP-TRE-CMV plasmid using the following oligonucleotides: Forward (For): AGCTTcg ATTTAAATatGGATCCtcTCTAGAgtCTCGAGatCCCGGGtcCATATGgtG;
Reverse (Rev): TCGACacCATATGgaCCCGGGatCTCGAGacTCTAGAgaGGAT CCatATTTAAATcgA.

pCS2^{+}-STOP-TRE-CMV-MCS (pCS2^{+}-STOP-TC)

The CMV promoter of pCS2+ was replaced with EcoRV-STOP-TRE-CMV-SwaI in SalI-HindIII after blunting of the ends.

Insertion of 2A sequence

To insert 2A sequence in ApaI site at 3' end, the H2BGFP fragment of 850bp was amplified by PCR from the plasmid pH2B-EGFP (Addgene) with a reverse primer with 2A-extention, and inserted in same plasmid in BamHI-XbaI site. Primers: For: AGGGTACTAAGGCCATCAC; Rev: TCTAGA-ta-GGG-CCC-TGG-GTT-GGA-CTC-CAC-GTC-TCC-CGC-CAA-CTT-GAG-AAG-GTC-AAA-ATT-CAA-AGT-CTG-TTT-CAC-CGG_CTTGTACAGCTCGTCCATG (ApaI site is underlined).

The blunted Sal-H2BGFP-2A-XbaI fragment was cloned into SwaI pKS-STOP-TC (pSTOP-TC-H2BGFP-2A(ApaI)). The same protocol was used to modified H2BGFP with 2A sequence bearing a HindIII site in the middle, in order to obtain the plasmid pH2BGFP-2A(HindIII). Primers: For: same primer; Rev: TCTAGA-ta-AAG-CTT-GAG-AAG-GTC-AAA-ATT-CAA-AGT-CTG-TTT-CAC-CGG_CTTGTACAGCTCGTCCATG (green: new triplet; HindIII site is underlined).

HcRed cDNA was amplified from the plasmid pLenti CMV H2B-HcRed-Hygro (Addgene) and a 2A sequence was cloned at 3'end. Two different strategies were used to insert ApaI or HindIII site at the end of 2A sequence. The primers used for amplification and modification of HcRed cDNA were: For: GCCGGC-at-ATGGTGAGCGGCCTGCTG; Rev1: GGG-CCC-TGG-GTT-GGA-CTC-CAC-GTC-TCC-CGC-CAA-CTT-GAG-AAG-GTC-AAA-ATT-CAA-AGT-CTG-TTT-CAC-CGG-GTTGGCCTTCTCGGGCAG (ApaI site is underlined); Rev2: AAG-CTT-GAG-AAG-GTC-AAA-ATT-CAA-AGT-CTG-TTT-CAC-CGG-GTTGGC CTTCTCGGGCAG (HindIII site is underlined). Amplicons were inserted at BamHI-HindIII sites or BamHI-ApaI sites in the plasmid Bluescript pKS, respectively. The final plasmids were named pKS-HcRed-2A(HindIII) and pKS-HcRed-2A (ApaI).

pTC_caALK5

Human caALK5 cDNA was amplified from pCMV_caALK5 (obtained from Wrama-Attisamo) and ApaI at 5' end and SalI at 3' end were inserted. The obtained amplicon was cloned in ApaI-KpnI (Blunt) pSTOP-TC-H2BGFP-2A (ApaI) to obtain the plasmid called pSTOP-TC-H2BGFP-caALK5 (pTC_caALK5).

pTC_caAlk3

Mouse caAlk3 cDNA was amplified from pCS2-caAlk3 (gift of professor S.Piccolo) with primers containing also the 2A sequence at 5' end and then substituted into the original plasmid between BamHI and NheI sites. Primers: For: GGATCC-ta-AAG-CTT-GCG-GGA-GAC-GTG-GAG-TCC-AAC-CCA-GGC-CCC-ATGACTCAGCTATACACTTCAT;Rev: CGTCTGGTAGATTTCTGTTTCT. HindIII-2A-caAlk3-XhoI fragment was cloned in HindIII-XhoI in pKS-HcRed-2A (HindIII). The final fragment BamHI-HcRed-2A-caAlk3-XhoI was inserted in pCS2^{+}-STOP-TRE-CMV-MCS between BamHI and XhoI.

pTC_Smad7

cDNA of mouse Smad7 was amplified from pBabe-Smad7 (Addgene) with this pair of primers: For: GGATCC-ta-AAG-CTT-GCG-GGA-GAC-GTG-GAG-TCC-AAC-CCA-GGC-CCC-ATGTTCAGGACCAAACGATCTG; Rev: GGAGGC GAGTAGGACGAGG. The final 2A (HindIII)-Smad7 was cloned in Bluescript pKS between BamHI and ApaI(Blunt). KpnI-HindIII fragment of H2BGFP-2A(HindIII) from pH2BGFP-2A(HindIII), was cloned in EcoRV-HindIII in pKS-2A(HindIII)-Smad7. The final fragment BamHI-H2BGP-2A-Smad7-XhoI was inserted in pCS2^{+}-STOP-TRE-CMV-MCS between BamHI and XhoI.

pTC_Smad6

cDNA of mouse Smad6 was amplified from pBabe-Smad6 (Addgene) with these pair of primers: For: GGATCC-ta-AAG-CTT-GCG-GGA-GAC-GTG-GAG-TCC-AAC-CCA-GGC-CCC-ATGTTCAGGACCAAACGATCTG; Rev: ACTCCGA CaCGGGCCTC. Final 2A (HindIII)-Smad6 was inserted in pBabe-Smad6 plasmid between BamHI and SalI. 2A-Smad6 HindIII-XhoI fragment was cloned in pKS-

HcRed-2A(HindIII). The final fragment BamHI-HcRed-2A-Smad6-XhoI was inserted in pCS2^{+}-STOP-TRE-CMV-MCS between BamHI and XhoI.

pTC_Noggin

Xenopus levis Noggin cDNA was amplified from pCMV_Noggin (gift of S.Piccolo lab), adding a ApaI site at 5' end and a SalI site at 3' end. Primers: For: GGGCCC-ATGGATCATTCCCAGTGCCTTGT; Rev: GTCCAG-TCAGCATGAG CATTTGCACTCGGA. The fragment ApaI-Noggin-SalI was inserted in ApaI-SalI in pKS-HcRed-2A(ApaI). The final fragment Not(Blunt)-HcRed-2A-Noggin-SalI was inserted in pCS2^{+}-STOP-TRE-CMV-MCS between SwaI-XhoI after blunting.

DNA fragments for microinjection were gel-purified and electroeluted in TAE 1X buffer.; then they were purified four times with phenol and once with chloroform. DNA was precipitated in EtOH and then re-suspended in microinjection buffer (Tris-HCl 10 mM, EDTA 0.1 mM pH 8). Another step of purification was made with *Bio-Spin 30 Chromatography Column* (Bio Rad), and then DNA fragments was filtered in Ultrafree Filter MC (0,22 µm, Millipore). Final concentration of DNA was about 1000 transgene copies per pl corresponding 2-5 ng/µl depending on the length of the fragment.

Reverse Transcriptase PCR (RT-PCR) analysis

RNA was extracted from normal and *Fbn1* mutant aortic arches of 2, 4 and 7-month-old mice, from aorta of doxycycline-treated mice or *in vitro* cultured VSMCs by TRIzol reagent (Gibco-BRL) as recommended by the manufacturer. RT-PCR analysis was performed as follows. First strand cDNA synthesis was performed using 1 µg total RNA and random hexanucleotides with SuperScriptIII reverse transcriptase (Invitrogen). The final solution of 20µl was diluted in 400µl of Nuclease-free water (Ambion). Real-Time PCR analysis was made with RotorGene RG-3000A (Corbett research) and analyzed by RotorGene3000 software. Amplification reaction was made in 15µl, containing 6µl of cDNA, 7,5µl of FastStartSyber Green Buffer (Roche), and 0,75µl of each primer. Each sample was analyzed in triplicate. The oligonucleotides used for these reactions are

reported in Table 2.1. To correct for sample variations in RT-PCR efficiency, the amplification of GAPDH gene was used as internal control.

Table 2.1. List of primer used for RT-PCR analyses

Target genes	Primer	Amplicon
PAI1	For:CCCTGGCCGACTTCACAA	79bp
	Rev:ACCTCGATCCTGACCTTTTGC	
Ctgf	For:AAGACACATTTGGCCCAGAC	497bp
	Rev:TTACGCCATGTCTCCGTACA	
Id1	For:CTGAACTCGGAGTCTGAAGT	125bp
	Rev:TCGTCGGCTGGAACACATG	
Id2	For:AAAACAGCCTGTCGGACCAC	121bp
	Rev:CTGGGCACCAGTTCCTTGAG	
Id3	For:AGCTTAGCCAGGTGGAAATCCT	121bp
	Rev:TCAGCTGTCTGGATCGGGAG	
GAPDH	For:ATCCTGCACCACCAACTGCT	119bp
	Rev:GGGCCATCCACAGTCTTGTG	
HcRed_caAlk3	For:GAGTACGGCAGCAGGACCTT	182bp
	Rev:CCGTGCACCTTCACCTTGTA	
HcRed_Noggin	For:CATCCTGCCAGAGGAGAGAC	122bp
	Rev:GAAGCCCCTCGTAAAACTCC	

Cell culture and transfection

Vascular Smooth Muscle Cells were purified from aorta of 1-month-old mice. After 90 minutes of Collagenase I digestion (Worthington), aortas were pelleted and then resuspended in Dulbecco's Modified Eagle's Medium (DMEM) containing 4.5g/L glucose, 25 mM Hepes, 2mM L-Glutamine (Invitrogen), supplemented with 20% Fetal Bovine Serum (FBS) (Invitrogen), 100 U/ml penicillin and 100 µg/ml streptomycin (Invitrogen).

HEK293T cells were cultured in Dulbecco's Modified Eagle's Medium (DMEM) containing 4.5g/L glucose, 25 mM Hepes, 2mM L-Glutamine (Invitrogen), supplemented with 10% Fetal Bovine Serum (Invitrogen), 100 U/ml penicillin and 100 µg/ml streptomycin (Invitrogen). Cells were maintained at 37°C in a humidified 5% CO_2 atmosphere. Cells were plated at 50% confluence on 60 mm diameter plates and transfected with the indicated plasmids using the calcium phosphate method (Sambrook et al., 1989). Briefly, the chosen DNA, dissolved in 250 mM $CaCl_2$, was added dropwise to an equal volume of 2x Hepes-buffered saline (HBS) (280 mM NaCl; 10 mM KCl; 1.5 mM Na2HPO4; 12 mM dextrose; 50 mM Hepes) with gentle mixing. Calcium phosphate-DNA solution was added dropwise to the Petri dish and immediately mixed by swirling. After 6-8 hours the culture medium was changed and incubation continued for additional 12-20 hours. Before harvesting, cells were cultivated in serum-free medium (OPTIMEM-Glutamax I, Invitrogen) for 36-48 hours.

Luciferase assay

HEK293T cells were transfected using the calcium phosphate method with the following plasmids: CAGA12-LUX reporter for TGF-β activity (gift from P. ten Dijke); pId1-Lux for BMP activity; pcDNA3-HASL-ALK5(TD) for expression of human caALK5 (obtained from Wrama-Attisamo); porcine constitutively active proTGF-$\beta1^{C223S/C225S}$ (gift from J.M. Davidson); mouse constitutively active Alk3 receptor (gift from S.Piccolo); pTetON for expression of rtTA (Clontech); transgenic plasmid pTC_caALK5, pTC_caAlk3, pTC_Smad7, pTC_Smad6 and pTC_Noggin; pCMV-LacZ (gift from S. Piccolo) for normalization for transfection

efficiency; expression plasmids coding for tested proteins. Cell layers were harvested with luciferase lysis buffer (25 mM Tris-HCl pH 7.8; 2.5 mM EDTA; 10% Glycerol; 1% NP40; 2 mM DTT) after 24 hours of starvation in DMEM supplemented with 0,1% FBS. Luciferase and β−galactosidase activity were measured in each sample and values of luciferase activity were normalized on β-galactosidase activity to account for differences of transfection efficiencies. Every sample was transfected in triplicate, and every experiment was repeated at least two times.

Genotype analysis

Genomic DNA was isolated from tail biopsies as described (Laird et al., 1991). The primer used for specific PCR reactions are reported in Table 2.2.

Table 2.2. List of primers used for PCR analysis of genotype

Mouse line	Primer to genotyping	Amplicon
Smmhc-rtTA	For: AATGGAGTCGGTATCGAAGG	361bp
	Rev: CCACGGCGGACAGAGCG	
TC_caALK5	For: CTAAGGATCCACCGGTCG	531bp
	Rev: GGCGGATCTTGAAGTTCACC	
TC_caAlk3	For: GTGAGCGGCCTGCTGAAG	674bp
	Rev: TTCTCGGGCAGGTCGCTG	
TC_Smad7	For: CTAAGGATCCACCGGTCG	531bp
	Rev: GGCGGATCTTGAAGTTCACC	
TC_Smad6	For: GTGAGCGGCCTGCTGAAG	674bp
	Rev: TTCTCGGGCAGGTCGCTG	
TC_Noggin	For: GTGAGCGGCCTGCTGAAG	674bp
	Rev: TTCTCGGGCAGGTCGCTG	
Smad4$^{f/f}$	For:GGGAAGCAAACAAAACAAGTC	wt: 249 bp floxed: 280 bp
	Rev:CAGAACAGATGTGCAATCGAA	
Fbn1$^{+/C1039G}$	For:TTGTCCATGTGCTTTAAGTAGC	After KpnI digestion: WT: 531 bp Mut: 531+335+245 bp
	Rev: ACAGAGGTCAGGAGATATGC	

Western blot analysis

Whole thoracic aortas dissected from 3-month-old *Smmh*-CreER^{T2};*Smad4*$^{f/f}$, *Smmh*-CreER^{T2} and wt mice after 15 days from tamoxifen treatment were cleaned from surrounding tissue and adventitia, snap frozen in liquid nitrogen, pulverized by a mortar and the powder was resuspended in lysis buffer (50 mM Hepes; 200 mM NaCl; 5 mM EDTA; 5% Glycerol; 1% NP40; 1x protease inhibitor cocktail (Roche); 1x phosphatase inhibitor cocktail (Sigma)). Protein content was determined by the BCA method (Pierce).

Aortic arches and thoracic aorta segments from 2, 4 and 7-month-old *Fbn1*$^{+/C1039G}$ and wt mice were frozen in liquid nitrogen, then proteins were extracted with "Total protein extraction kit" (Millipore). Protein content was determined by the BCA method (Pierce).

Samples from transfected HEK293T cells were collected in ice-cold NP40 lysis buffer (25 mM Tris-HCl pH 7.5; 2.5 mM EDTA; 1% NP40; 1x protease inhibitor cocktail). Sample loading was normalized for differences of transfection efficiency on the basis of β-galactosidase activity.

Protein samples were resolved under reducing conditions by SDS-PAGE in 4-12 or 10% NuPAGE® Bis-Tris gels (Invitrogen) and blotted onto polyvinylidene difluoride membranes (Millipore). Filters were blocked with 5% non-fat dry milk (Biorad) in TBS 1x (TBS 10x: 80 g Tris; 24.2 g NaCl in 1 liter) containing 0.1% Tween20 (TBS-T) buffer and then incubated with the primary antibodies. Following washes with TBS-T buffer, the membranes were incubated with horseradish peroxidase-linked secondary antibodies (Amersham Bioscience) and reacting bands revealed with SupersignalWest-pico and -dura HRP substrates (Pierce). Primary antibodies used were: monoclonal mouse anti-Smad4 (Santa Cruz), 1:1000 dilution; monoclonal mouse anti-GAPDH (Millipore), 1:6000 dilution; rabbit polyclonal against P-Smad2/3 (Cell signalling), 1:1000 dilution; rabbit polyclonal against P-Smad1/5/8 (Millipore), 1:1000.

Southern blot analysis

Approximately 7 µg of genomic DNA was cut with the appropriate restriction enzyme, loaded onto an 1% agarose gel and run in 1x TAE buffer. The gel was then removed and incubated for 30 min in a solution of 0.4 M NaOH at room temperature. During this incubation, a blot chamber was set up. A Tupperware box was filled with transfer buffer (0.4 M NaOH) and a platform was then prepared by covering it with Whatman 3MM filter paper soaked in 0.4 M NaOH. The gel with wells facing up was carefully laid down and covered with Gene Screen Plus nylon membrane (PerkinElmer Life Sciences), cut to gel size and previously equilibrated for 20 min in 0.4 M NaOH solution. The transfer was allowed to continue overnight by capillary forces. The nylon membrane was then removed, washed in 0.4 M NaOH for 5 min, dried at room temperature and DNA fixed by a UV cross- linker (Bio Rad). Pre-hybridization was carried out for 30' at 42°C in ULTRAhyb-oligo (Ambion). After addition of the appropriate radiolabeled probe (final concentration 3.3 ng/ml, 5.1x106 cpm/ml), hybridization was performed overnight at 42°C in a hybridization oven (Bachofer). The membrane was then washed three times as follows: *i)* 10 min at room temperature in 2x SSC and 1% SDS; *ii)* 10 min at room temperature in 1x SSC and 0.5% SDS; *iii)* 5 min at 65°C in 0.2x SSC and 0.5% SDS. The membrane was finally rinsed in 2x SSC and subjected to autoradiography with X-Omat (Kodak) films.

Immunofluorescence

Aortic portions were embedded in OCT (Sakura), frozen in liquid nitrogen cold isopentane and stored at -80°C. Cryosections (7 µm thick) were collected on positively charged slides (BDH Superfrost Plus), air dried at room temperature and kept at -80°C. Before being used, the sections were equilibrated at room temperature and hydrated with phosphate-buffered saline (PBS) for 5 min. Then the sections were saturated with the blocking buffer (10% goat serum in PBS) for 30 min. Primary and secondary antibodies were diluted in 5% goat serum. The antibodies used were the following: polyclonal rabbit anti-Smad4 (Santa-Cruz); goat anti-rabbit IgG Cy3-conjugated antibody (Jackson Immuno Research).

Slides were incubated for 2 h at room temperature or overnight at 4°C with the primary antibody. Secondary antibody was applied for 1 h at room temperature. The slides were mounted in 80% glycerol in PBS and observed in a Bio-Rad confocal microscope.

Histological analyses

To perform histological staining, thoracic and abdominal aortas from selected experimental mice were fixed with 4% paraformaldehyde overnight, dehydrated through successive steps on solutions of increasing concentrations of ethanol and embedded in paraffin. 7 µm sections were stained with Hematoxylin & Eosin and Weigert's stain following established procedures. The slide were observed using a Zeiss Axioplan microscope equipped with a Leica DC 500 digital camera.

TUNEL assay

To detect apoptotic nuclei, aortas of *Smmhc*-CreER^{T2}*;Smad4*$^{f/f}$ were fixed with 4% paraformaldehyde overnight, dehydrated through successive steps on solutions of increasing concentrations of ethanol and embedded in paraffin: 7 µm thick paraffin sections were prepared and subjected to the TUNEL procedure.

The sections were laid on positively charged slides (BDH Superfrost Plus, deparaffinized, rehydrated and washed in PBS before being subjected to the procedure using the TUNEL kit "ApopTag Tunel" (Intergen). The sections were treated with proteinase K for 15 minutes, in order to expose the DNA sites recognized by the enzyme, washed in PBS, and then with H_2O_2 to saturate in order to inhibit possible endogenous peroxidases. After pre-incubation with *TUNEL reaction buffer*, the section were incubated with enzyme TdT and digoxigenin-labeled nucleotides for 1 hour at 37°C. After three washes with PBS, an incubation was performed with an anti-digoxigenin secondary antibody conjugated to peroxidase. The peroxidase reaction was developed providing carbazole as substrate, dissolved in acetate buffer and H_2O_2. After staining of the nuclei with Hoechst 33258 (Sigma) and the washes in PBS and water, the slides

were finally mounted with 80% glycerol in PBS. The number of total and TUNEL-positive nuclei was determined in at least 20 randomly selected fields using a Zeiss Axioplan microscope equipped with a Leica DC 500 digital camera.

Echocardiograph analysis and measurement

All echocardiograms were performed on sedated mice following removal of hair by Nair ® hair removal cream using the VisualSonics Vevo 2100 imaging system and the MS550D transducer (22-55 MHz). The aorta was imaged using a parasternal long axis view. The physiological parameters of the animals were continuously monitored and registered. Three separate measurements of the maximal internal systolic dimension at the Sinus of Valsalva were made and the mean of measures was calculated.

Statistical analysis

Wall thickness, internal circumference, islands of damage and aortic dilatation were measured on sections taken from two mice. For wall thickness, at least 6 measurements were taken in each section and at least 8 sections were considered. Data were analyzed by a one-way ANOVA and Tukey post-hoc test. The results are expressed as mean ± SEM. A P value <0.05 was assigned statistical significance. For luciferase assay and RT-PCR, data are expressed as mean ± SD. The statistical significance of the results was determined by using Student's t-test. A P value <0.05 was considered significant.

RESULTS

Activation of TGF-β growth factors signaling in aorta of Fbn1$^{+/C1039G}$ mice

Analysis of Smads phosphorylation

As first step of our study on the role of growth factors of the TGF-β family in the development of TAA in the mouse model of Marfan syndrome, the activation of TGF-β and BMP signaling was assessed in aorta of *Fbn1* mutant mice, analyzing Smads phosphorylation (P) levels at different age using Western blotting. The analysis was carried out separately in the aortic arch, the site where aneurysms form in the *Fbn1*$^{+/C1039G}$ mutant, and in descending/thoracic aorta, a region where morphological alterations of arterial wall are mild or absent (Judge et al., 2004). In aortic arch, P-Smad1/5/8, an indicator of BMP signaling, was increased in *Fbn1* mutants at 2 and 4 months, but not at 7 months, compared to age-matched controls (Fig. 3.1A; *Fbn1*$^{+/C1039G}$ 2 months 1,5 +/- 0,1; 4 months 1,9 +/- 0,2; 7 months 0,9 +/- 0,1 fold). At the same age, *Fbn1* mutant mice showed also increased P-Smad2/3 levels in aortic arch, excepting 7-month-old mice (Fig. 3.1B; *Fbn1*$^{+/C1039G}$ 2 months 2,9 +/- 0,5; 4 months 1,7 +/- 0,2; 7 months 0,9 +/- 0,1 fold). The latter observation is in contrast with data reported in the literature for older mice (Holm et al., 2011). In descending aorta P-Smad1/5/8 was increased in *Fbn1* mutant at 2 and 4 months, as observed in aortic arch, compared to controls (Fig. 3.1C; *Fbn1*$^{+/C1039G}$ 2 months 1,28 +/- 0,1; 4 months 1,55 +/- 0,2; 7 months 1,07 +/- 0,1 fold). Moreover the same trend was observed for phosphorylation of Smad2/3 in *Fbn1* mutants (Fig. 3.1D; *Fbn1*$^{+/C1039G}$ 2 months 1,25 +/- 0,1; 4 months 1,72 +/- 0,2; 7 months 1,01 +/- 0,1 fold).

Analysis of P-Smads levels indicates that activation of TGF-β and BMP signaling is not confined in the arch region, where aneurysm develops, but is present in the whole aorta of *Fbn1* mutant mice.

Analysis of TGF-β and BMP target genes expression in aorta of mutant mice

Growth factors of the TGF-β family induce functional effects by altering gene expression. To investigate whether increased P-Smads in mutant aorta influenced the genetic program of cells, target genes expression was investigated by real-time RT-PCR. Genes analyzed included PAI-1 and Ctgf which are frequently associated with increased Smad2/3 phosphorylation (Velasco et al., 2008; Holm et al., 2011; Neptune et al., 2003), and Id1-2-3 transcription factors that are regulated by BMP. Surprisingly, in aortic arch, Ctgf expression was increased not only at 2 months, when higher levels of P-Smad2/3 were detected, but also at 7 months, when no variation of phosphorylation of Smad2/3 was apparent (Fig. 3.2B and Fig. 3.1B). Moreover, both Ctgf and PAI-1 genes were induced at 7 months, an age in which aortic aneurysm was present, but we did not register increased TGF-β signaling (Fig. 3.2B and Fig. 3.1B). Characterization of BMP target genes revealed increased expression of Id2 and Id3, but not Id1, in younger *Fbn1* mutant mice. At 7 months, while the relative amount of Id3 mRNA remained higher in mutant compared to wild-type animals, this was not the case for Id2, whose expression in mutant mice decreased to control levels (Fig. 3.2A).

Real-time RT-PCR analysis in thoracic aorta of *Fbn1* mutants and controls revealed differences also in this aortic tract. Ctgf expression was elevated at 2 months but not at 7 months in *Fbn1* mutants (Fig. 3.2D), while there was no variation of PAI1 expression at all ages, even if increase of P-Smad2/3 level was detected (Fig. 3.1D and Fig. 3.2D). In thoracic aorta, analysis of BMP target genes induction showed increased Id2 and Id3 expression, but not Id1, in 2-month-old *Fbn1* mutants (Fig. 3.2C), while no variation of all Id isoforms was detected at 7 months (Fig. 3.2C).

Overall, it can be noted that data on target genes expression (Fig. 3.2) are difficult to reconcile with those on growth factors signaling based on P-Smads analysis (Fig. 3.1). While an exhaustive examination of this problem is given in the Discussion, data suggest that progression of aortic arch aneurysm in *Fbn1*$^{+/C1039G}$ mice is a complex process, likely involving other pathways in addition to those regulated by growth factors of the TGF-β family.

Generation of transgenic mice to modulate levels of TGF-β and BMP signaling

One of the aims in this study is to investigate the role of TGF-β/BMP activation or inhibition in the development of aortic aneurysms in *Fbn1*$^{+/C1039G}$ mutant mice. To this purpose, we used an inducible gene expression method based on the Tet-On system (Clontech) that uses the reverse tetracycline transactivator (rtTA) to activate gene expression in the presence of doxycycline. To restrict modulation of TGF-β/BMP signaling only in VSMCs, the main cell type affected by the Fibrillin-1 mutations in Marfan syndrome (Nataatmadja et al., 2006; Carta et al., 2009), rtTA expression was put under the control of the smooth muscle myosin heavy chain promoter (Fig. 3.3B).

Five polyprotein constructs expressing specific cDNAs under a TRE-CMV minimal promoter were generated. cDNAs coding for constitutively active (ca) forms of TGF-β receptor I (caALK5) and for Alk3 BMP receptor (caAlk3) allowed for increase of TGF-β and BMP signaling. Instead, an inhibitory effect on BMP or TGF-β signaling was obtained using cDNAs for inhibitory Smad6 and Smad7 respectively, or Noggin, an inhibitor of all BMP isoforms. All the constructs, also carried the cDNA for a reporter gene: a histone H2B-green fluorescent protein fusion (H2BGFP) was used as reporter for cDNAs modulating the TGF-β pathway (caALK5 and Smad7), while HcRed was associated with cDNAs regulating the BMP pathway (caAlk3, Smad6 and Noggin) (Fig. 3.3A). To obtain the simultaneous expression of the two proteins encoded in each construct, a 2A viral sequence from Foot and Mouth Disease virus was inserted between the two cDNAs. 2A is a sequence of 54 bp, coding for 18 aa in which the C-terminal amino acids are GPG. The cDNA sequence coding for the two proteins (polyprotein) is transcribed into a unique mRNA molecule that is normally recruited by the translation machinery. During the translation process, a cleavage occurs between the proline and the second glycine of the GPG sequence, causing release of the first protein with the 2A sequence at the C terminus (Donelly et al., 2001). This processing does not interrupt translation that continues up to the completion of the second protein (Donelly et al., 2001).

To test the effective function of this inducible polyprotein self-processing system, plasmid constructs were transfected into HEK293T cells, together with

the rtTA coding plasmid. After treatment with doxycycline, a luciferase reporter assay was used to check activation or inhibition of TGF-β and BMP signaling (Fig. 3.4A-D). As expected, substantial activation of TGF-β signaling was observed only after expression of caALK5 in the presence of co-transfected rtTA and of doxycycline (Fig. 3.4A); similarly, inhibition was detected after co-transfection of ca-proTGF-β1$^{C223S/C225S}$ and pTC_Smad7 (Fig. 3.4B). Moreover, reduction of BMP reporter signal was the result of Smad6 and Noggin expression (Fig. 3.4C-D), while increased phosphorylation of Smad1/5/8 was detected after transfection of pTC_caAlk3 (Fig. 3.4E). Together with the expected activation/inhibition of TGF-β or BMP signaling, expression of reporter proteins H2BGFP (nuclear) and HcRed (cytoplasmic) was also detected (Fig. 3.4F-I). All polyprotein coding constructs were used to generate transgenic mice by pronuclear microinjection, as reported in Table 3.1. One transgenic mouse line expressing the rtTA driver only in smooth muscle cells was obtained by oocyte microinjection of a BAC clone modified by recombineering method to insert rtTA cDNA at the first codon of the smooth muscle myosin heavy chain (*Smmhc*) gene (Fig. 3.3B). Integration and integrity of BAC clone in mouse genome was checked by Southern Blotting (Fig. 3.3C).

Table 3.1 Generation of transgenic mouse line with inducible gene system.

Construct	N° of transferred zigotes	Born animals	N° of founders	Efficiency
pTC_caALK5	286	90	5	5,5 %
pTC_Smad7	216	86	2	2,3 %
pTC_caAlk3	288	90	3	3,3 %
pTC_Noggin	232	89	3	3,3 %
pTC_Smad6	270	101	2	2,0 %

Testing appropriate function of the transgenic inducible system

To test the appropriate function of the designed inducible system, the driver transgenic mouse line *Smmhc*-rtTA (Fig. 3.3B) was crossed with transgenic lines positive for the responsive constructs (Fig. 3.3A and Table 3.2) and aorta (or derived primary cell cultures) from the resulting double transgenic lines was examined using different methods. VSMCs cultures derived from *Smmhc*-rtTA;TC_caAlk3 mice were analyzed first. Cells were treated with different concentrations of doxycycline (1-100 µg/ml) for 48hs, and activation of the transgene was detected by real time RT-PCR. Induction of transgene expression was negligible at 1-10 µg/ml, but high at 100 µg/ml doxycycline (Fig. 3.5A). A functional effect of the production of constitutively active BMP receptor I was indicated by the parallel induction of BMP target genes Id1-2-3 only in VSMCs treated with 100 µg/ml of the drug (Fig. 3.5B; Id1 2,8 fold; Id2 2,5 fold; Id3 2 fold). We next investigated transgene induction *in vivo* by treating double transgenic *Smmhc*-rtTA;TC_caAlk3 mice with 1mg/ml of doxycycline in drinking water for 30 and 60 days. RT-PCR analysis of aorta RNA after 30 days indicated no transgene induction and no differences in Ids expression between treated and untreated *Smmhc*-rtTA;TC_caAlk3 mice (data not shown). However, an induction of 4,2 and 18,12 fold was observed in caAlk3 mRNA levels in two double transgenic mice compared to untreated controls at 60 days (Fig. 3.5C). Interestingly the two *Smmhc*-rtTA;TC_caAlk3 treated mice showed a parallel increase of Id2 expression (1,72 and 3,3 fold in the two mice) (Fig. 3.5D). Taken together, the data indicate that the designed inducible system works correctly in aorta, showing low levels of transgene expression in the absence of the inducing drug and considerable induction after doxycycline administration. The lack and presence of transgene induction at 30 and 60 days respectively, suggest that doxycycline treatment *in vivo* requires a lag time for effective regulation of inducible genes.

Characterization of transgene induction *in vivo* was also carried out in a different line of double transgenic mice, *Smmhc*-rtTA;TC_Noggin. In this experiment, animals were treated for 15 days with a higher concentration of doxycycline (10 mg/ml) before RT-PCR analysis. Data revealed induction of

Noggin expression of 3,5 fold in *Smmhc*-rtTA;TC_Noggin treated compared to untreated mice (Fig. 3.5E). As Noggin is a BMP inhibitor, the expected effect of its expression is reduction of BMP signaling and of BMP target genes. RT-PCR analysis didn't reveal significant difference in Ids expression between double transgenic treated and untreated mice (data not shown). However, this result may be the consequence of the difficulty of detecting reduction of expression of genes, whose mRNA levels are usually low, rather than implying that Noggin expression was ineffective (see Discussion for a complete argumentation of this point). Actually, the additional double transgenic mouse lines (*Smmhc*-rtTA;TC_caALK5, *Smmhc*-rtTA;TC_Smad6, *Smmhc*-rtTA; TC_Smad7) are under doxycycline treatment for similar characterization of transgene induction. Moreover, the increasing availability of double transgenic mice will allow application of further assays, such as the detection of P-Smads levels, for full characterization of the inducible system used.

Table 3.2: Crossings of transgenic mouse lines planned to modulate TGF-β and/or BMP signaling in aorta VSMCs

Crosses of transgenic mice	Expected effect on signaling
Smmhc-rtTA x TC_caALK5	⇧ TGF-β
Smmhc-rtTA x TC_caAlk3	⇧ BMP
Smmhc-rtTA x TC_caALK5;TC_caAlk3	⇧ TGF-β, ⇧ BMP
Smmhc-rtTA x TC_Smad7;TC_caAlk3	⇩ TGF-β, ⇧ BMP
Smmhc-rtTA x TC_caALK5;TC_Noggin	⇧ TGF-β, ⇩ BMP
Smmhc-rtTA x TC_caALK5;TC_Smad6	⇧ TGF-β, ⇩ BMP
Fbn1$^{+/C1039G}$ x *Smmhc*-rtTA;TC_Noggin	⇩ BMP
Fbn1$^{+/C1039G}$ x *Smmhc*-rtTA;TC_Smad7	⇩ TGF-β
Fbn1$^{+/C1039G}$ x *Smmhc*-rtTA;TC_Smad6	⇩ BMP

Analysis of the role of TGF-β/BMP signaling in the progression of the Marfan-like phenotype of adult Fbn1$^{+/C1039G}$ mutant mice

Conditional inactivation of the TGF-β/BMP downstream effector Smad4 in adult mice

Although it is well established that TGF-β signaling is upregulated in Marfan patients (Nataatmadja et al., 2006; Matt et al., 2009) and in animal models of the disease (Carta et al., 2009; Habashi et al., 2006 and this thesis), the role of this enhanced TGF-β activity in aneurysm formation and progression is still uncertain. On one hand, inhibition of signaling by administration of neutralizing antibodies to TGF-β retarded TAA formation (Habashi et al., 2006) in *Fbn1$^{+/C1039G}$* mice, but, on the other, inactivation of one allele of *Smad4*, a downstream effector in the TGF-β and BMP pathway, accelerated the progression of aneurysm in the same animal model (Holm et al., 2011). The latter study, however, was conducted on *Fbn1* mutants heterozygous for a null mutation of *Smad4* (homozygous null is embryonic lethal), thus raising the possibility that reduced TGF-β/BMP signaling during development may have induced alterations of aorta VSMCs favoring aneurysm progression in adult animals. To rule out this possibility, the role of TGF-β growth factors activity in aneurysm formation was investigated in a conditional transgenic model, in which *Smad4* inactivation was induced in adult mice that developed normally (Fig. 3.6A).

3-month-old *Smmhc*-CreER^{T2}*;Smad4$^{f/f}$* mice, and age matched controls, were treated with tamoxifen for 10 days to activate the CreER^{T2} recombinase. This treatment was sufficient to completely inactivate *Smad4* expression, as revealed by the considerable reduction of Smad4 detected by Western Blot analysis in aorta extracts (Fig. 3.6B). This was confirmed by lack of Smad4 immunofluorescence staining in the media of aorta from *Smmhc*-CreER^{T2}*; Smad4$^{f/f}$* mice after tamoxifen treatment (Fig. 3.6C).

Aortic alterations induced by Smad4 conditional knockout

Morphological analysis of aortic arch was carried out on *Smmhc*-CreER^{T2}*; Smad4$^{f/f}$* mice at 9 weeks from the beginning of treatment with tamoxifen. As controls, wild-type mice carrying the *Smmhc*-CreER^{T2} transgene were used. H&E staining of aorta did not show any obvious modification compared to controls at 9 weeks (Fig. 3.7A and Fig. 3.7B). On the other hand, interruptions of the continuity of elastic lamellae become apparent with Weigert staining (Fig. 3.7D and Fig. 3.7E). After 5 months from the beginning of treatment, aortic arch of *Smmhc*-CreER^{T2}*;Smad4$^{f/f}$* mice showed increased vessel damage, with increase of elastic lamellae ruptures (Fig. 3.7F). Moreover, although there was no change in vessel wall thickness (data not shown), we registered an increase of perimeter of internal elastic lamellae (IEL) (Fig. 3.7G), and of suffering of VSMCs as observed by count of apoptotic cells with TUNEL assay (Fig. 3.7I-M). *Smad4* knockout also affected survival of animals that died for aortic dissection usually between 4 and 6 months after treatment (Fig. 3.7H). Inflammatory cells were not present in the vessel wall and were only observed around the site of dissection (data not shown).

Worsening of aneurysm progression in Fbn1$^{+/C1039G}$ mice by inhibition of TGF-β/BMP signaling in VSMCs

It has been reported recently that *Smad4* haploinsufficiency in *Fbn1$^{+/C1039G}$* mice promotes diffusion of aneurysm from aortic root to ascending tract and increases frequency of premature death due to thoracic aortic dissection (Holm et al., 2011). This observation suggests a protective role for canonical TGF-β/BMP signaling in Marfan syndrome, at variance with the diffused view that TGF-β activation is instrumental for development of aortic alterations (see Introduction). However, it should be noted that the Holm's et al. data were obtained using *Smad4$^{+/-}$* mice with a null mutation, so that the results may have been influenced by alterations of the function of other affected tissues in addition to the vessel media, or by abnormalities brought about by interference of normal embryonic development after decreased dosage of TGF-β/BMP signaling. To overcome

these difficulties, tissue specific inactivation of *Smad4* was carried out in adult mice by crossing the *Fbn1*$^{+/C1039G}$ and the *Smmhc*-CreER^{T2};*Smad4*$^{f/f}$ lines. 5-month-old *Smmhc*-CreER^{T2};*Smad4*$^{f/f}$;*Fbn1*$^{+/C1039G}$ mice, and age match controls, were treated with tamoxifen for 10 days and aneurysm progression was monitored by echocardiograph measurement of aortic root diameter at different times. Just before treatment (t0), *Fbn1*$^{+/C1039G}$ and *Smmhc*-CreER^{T2}; *Smad4*$^{f/f}$;*Fbn1*$^{+/C1039G}$ mice showed aortic root dilatation, while root diameter of *Smmhc*-CreER^{T2};*Smad4*$^{f/f}$ animals was similar to controls (wt 1,63 +/- 0,04 mm; *Smmhc*-CreER^{T2};*Smad4*$^{f/f}$ 1,75 +/- 0,03 mm; *Fbn1*$^{+/C1039G}$ 2,45 +/- 0,06 mm; *Smmhc*-CreER^{T2};*Smad4*$^{f/f}$; *Fbn1*$^{+/C1039G}$ 2,46 +/- 0,02 mm) (Fig. 3.8A-D and Fig. 3.8I). On the contrary, mice carrying both *Fbn1* and *Smad4* mutations exhibited more severe dilatation of aortic root than *Fbn1*$^{+/C1039G}$ after 45 days from start of tamoxifen administration, while the diameter measured in *Smad4*$^{f/f}$ did not differ from that of control mice (wt 1,67 +/- 0,05 mm; *Smmhc*-CreER^{T2};*Smad4*$^{f/f}$ 1,70 +/- 0,05 mm; *Fbn1*$^{+/C1039G}$ 2,54 +/- 0,03 mm; *Smmhc*-CreER^{T2};*Smad4*$^{f/f}$; *Fbn1*$^{+/C1039G}$ 2,75 +/- 0,05 mm) (Fig. 3.8E-H and Fig. 3.8I). The enlargement of aortic root following tamoxifen treatment is clearly appreciated considering the aortic root growth: this was similar in animals with *Smad4* or no mutation and twice and six times this value in *Fbn1* and double mutants, respectively (Fig. 3.8J). Thus, strong inhibition of TGF-β/BMP signaling, as achieved in the transgenic mouse model used here, considerably aggravates progression of aortic arch aneurysms. A similar effect was not observed by Holm and colleagues in *Smad4*$^{+/-}$; *Fbn1*$^{+/C0139G}$ mice, likely because halving gene dosage of *Smad4* is not sufficient to induce detectable alterations in aorta.

Inhibition of Smad4 function in Fbn1 mutant mice induces a severe aortic dissection phenotype and the appearance of abdominal aortic aneurysms

In *Fbn1*$^{+/C1039G}$ mice, aneurysm rupture is very rare; this event, however, became frequent by halving the *Smad4* gene dosage (about 50% survival at 5 months) (Holm et al., 2011). As reduction of *Smad4* achieved in the transgenic mice used in this study is much higher (Fig. 3.6B), an increased frequency of aortic dissection was expected. In our experiments, a total of four *Smmhc*-

CreER^{T2};*Smad4$^{f/f}$;Fbn1$^{+/C1039G}$* mice (two 2-month-old and two 5-month-old), together with a similar number of age-matched controls, were used. All four double transgenic animals died within two months from beginning of tamoxifen treatment, while all animals of the other experimental groups survived to this age (Fig. 3.9A and Fig. 3.9B). Necropsy revealed the intriguing finding that abdominal aneurysms had developed in these animals. The two 5-month-old *Smmhc*-CreER^{T2};*Smad4$^{f/f}$;Fbn1$^{+/C1039G}$* mice died for dissection of abdominal aortic aneurysm (AAA) and thoracic aortic aneurysm (TAA), respectively. Both animals showed TAA (Fig. 3.10A-D, blue arrow), but only one had AAA (Fig. 3.10A-D, red arrow). Macroscopically, *Smmhc*-CreER^{T2};*Smad4$^{f/f}$;Fbn1$^{+/C1039G}$* aortic arch showed severe TAA compared to age matched *Fbn1$^{+/C1039G}$* controls and diffusion of aneurysm also in ascending tract of aorta (Fig. 3.10E-H, blue arrow). Histological analysis of TAA sections with Weigert staining revealed increased damage of elastic lamellae in *Smmhc*-CreER^{T2};*Smad4$^{f/f}$;Fbn1$^{+/C1039G}$* aortic arch, characterized by higher number of elastic fibers ruptures and increased matrix deposition, compared to *Fbn1$^{+/C1039G}$* controls (Fig. 3.10I-L). Although *Smmhc*-CreER^{T2};*Smad4$^{f/f}$;Fbn1$^{+/C1039G}$* mice presented vessel wall thickness comparable to *Fbn1$^{+/C1039G}$* controls (Fig. 3.12A), they showed higher number of islands of damage (elastic lamellae ruptures and matrix deposition) compared to *Fbn1$^{+/C1039G}$* mice. Worth of note, islands of damage were also observed in *Smmhc-CreER^{T2};Sma4$^{f/f}$* mice, while they were rarely found in wt controls (Fig. 3.12C ; wt 0,4+/-0,4, *Fbn1$^{+/C1039G}$* 11,6 +/- 0,7, *Smmhc*-CreER^{T2};*Smad4$^{f/f}$* 4,2 +/- 0,4, *Smmhc*-CreER^{T2};*Smad4$^{f/f}$;Fbn1$^{+/C1039G}$* 21,5 +/- 1).

As reported in literature, disarray of elastic lamellae was observed in aortic arch of the mouse model of Marfan syndrome (Judge at al., 2004; Habashi et al., 2006; Holm et al., 2011; Fig. 3.10I-J), while abdominal aorta segment was normal. Also, in our study we did not observe alterations in abdominal aortic section of *Fbn1$^{+/C1039G}$* mice, compared to wt age-matched controls (Fig. 3.11E and Fig. 3.11F). On the contrary, severe damage of aortic abdominal wall, characterized by elastic lamellae ruptures and abnormal matrix deposition, was found in *Smmhc*-CreER^{T2};*Smad4$^{f/f}$;Fbn1$^{+/C1039G}$* double mutants (Fig. 3.11H). Moreover, *Smmhc*-CreER^{T2};*Smad4$^{f/f}$;Fbn1$^{+/C1039G}$* had increased wall thickness (Fig. 3.12B; wt 46,14 +/- 1,2 µm, *Fbn1$^{+/C1039G}$* 45,84 +/- 1,0 µm, *Smmhc*-

CreER^{T2};*Smad4*$^{f/f}$ 44,15 +/- 1,1 μm, *Smmhc*-CreER^{T2};*Smad4*$^{f/f}$;*Fbn1*$^{+/C1039G}$ 60,35 +/- 1,3 μm), internal aortic circumference (Fig. 3.12D; wt 1800 +/- 66 μm, *Fbn1*$^{+/C1039G}$ 2381 +/- 54 μm, *Smmhc*-CreER^{T2};*Smad4*$^{f/f}$ 2254 +/- 53 μm, *Smmhc*-CreER^{T2};*Smad4*$^{f/f}$;*Fbn1*$^{+/C1039G}$ 2820 +/- 75 μm) and islands of damage (Fig. 3.12C) compared to controls.

Considering the results obtained with the 2-month-old animals, it should be noted that morphology of aortic arch was normal at this age (Judge et al., 2004). However, a different result was obtained after *Smad4* inactivation in 2-month-old *Smmhc*-CreER^{T2};*Smad4*$^{f/f}$;*Fbn1*$^{+/C1039G}$ mice, in which there was no evidence of aneurysm before tamoxifen administration. The two *Smmhc*-CreER^{T2}; *Smad4*$^{f/f}$;*Fbn1*$^{+/C1039G}$ mice studied died at 25 and 45 days from the beginning of tamoxifen treatment for abdominal aortic aneurysm dissection. At necroscopy aortas presented also enlarged TAA compared to age-matched *Fbn1*$^{+/C1039G}$ (Fig. 3.13A-C) and AAA (Fig. 3.13A, Fig. 3.13D and 3.13E). No changes were observed in wt and *Smmhc*-CreER^{T2};*Smad4*$^{f/f}$ (data not shown), but wall damage was evidenced in both arch and abdominal segments of *Smmhc*-CreER^{T2};*Smad4*$^{f/f}$;*Fbn1*$^{+/C1039G}$ mice (Fig. 3.13F and Fig. 3.13G).

Detailed histological analysis was carried out in serial sections of aortic arch and abdominal aorta of two *Smmhc*-CreER^{T2};*Smad4*$^{f/f}$;*Fbn1*$^{+/C1039G}$ mice that were 2- and 5-month old at the moment of tamoxifen administration and that died by abdominal dissection after 25 and 53 days, respectively, from start of treatment. In both aortic arch and abdominal aorta, a focal site of inflammatory infiltration was observed in the adventitial layer. The underlying media was severely altered and infiltrated only at sites of rupture of aneurysms, while it maintained an apparent normal morphology and absence of infiltration elsewhere (Fig. 3.13H, Fig. 3.13I, Fig. 3.10M-P and Fig. 3.11I-L). The morphological analysis suggests that inflammation of aortic arch and abdominal aorta initiates at discrete sites and then may deepen slowly into the media, while most aortic media, even if showing elastic fiber ruptures and islands of damage, is not interested by the inflammatory process. The impression coming from these limited observations is that inflammation is not relevant for the structural alterations of the aortic wall induced by *Fbn1* and *Smad4* mutations, but may be important in accelerating the process of aneurysm dissection.

FIGURES

Figure 3.1. Activation of TGF-β growth factors signaling in *Fbn1*$^{+/C1039G}$ mice. A-D) Detection of P-Smads in aorta of wild-type and *Fbn1* mutant mice at 2, 4 and 7 months. *Fbn1* mutants showed increased P-Smad1/5/8 (A,C) only at 2 and 4 months (m), in both aortic arch (A) and thoracic aorta (C). P-Smad2/3 levels were higher in aortic arch and thoracic aorta of mutants at 2 and 4 months (B, D). *, P< 0,05; NS, not significant.

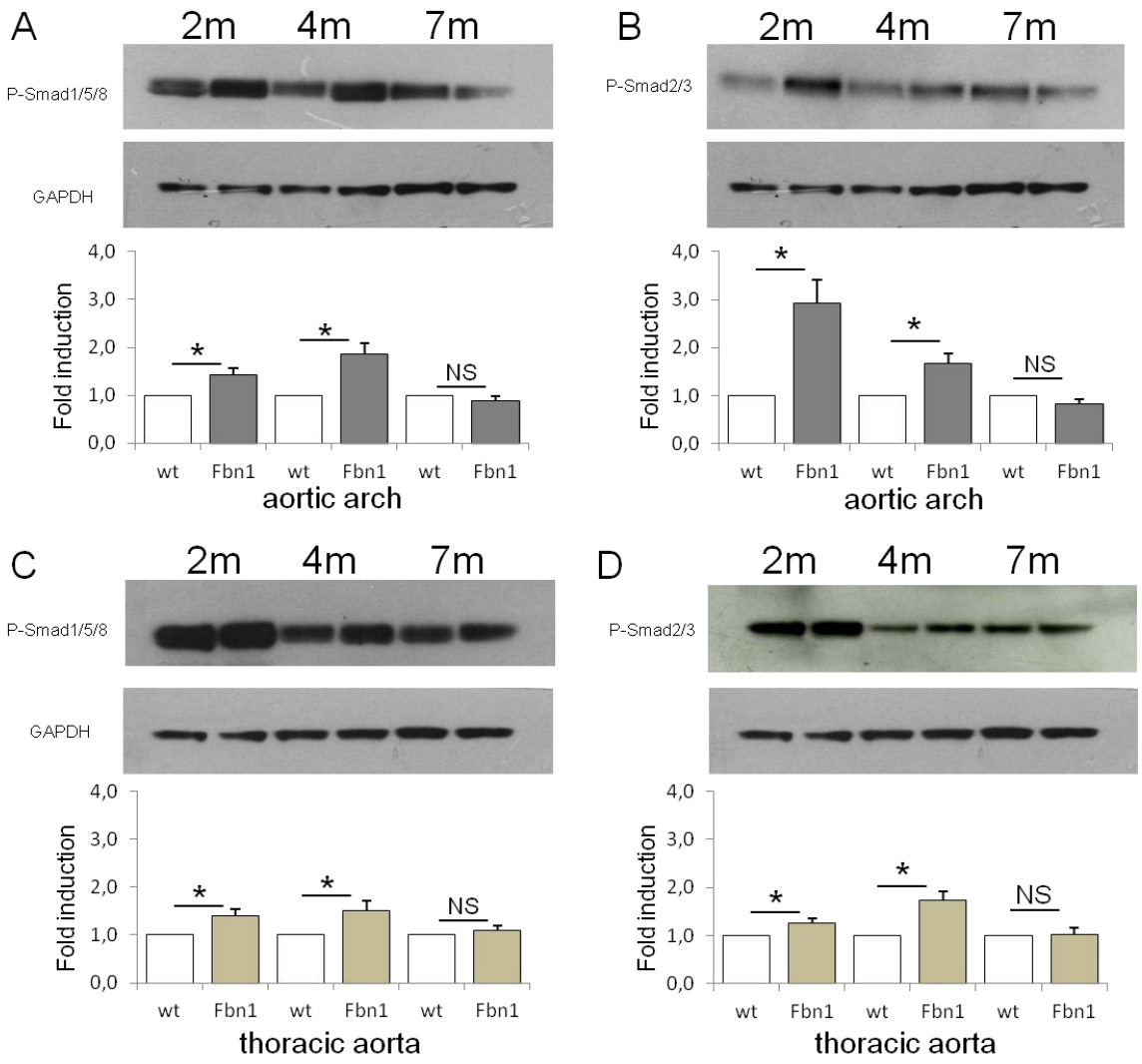
A
2m
4m
7m
P-Smad1/5/8
GAPDH
Fold induction
4,0
3,0
2,0
1,0
0,0
*
*
NS
wt
Fbn1
wt
Fbn1
wt
Fbn1
aortic arch
B
2m
4m
7m
P-Smad2/3
Fold induction
4,0
3,0
2,0
1,0
0,0
*
*
NS
wt
Fbn1
wt
Fbn1
wt
Fbn1
aortic arch
C
2m
4m
7m
P-Smad1/5/8
GAPDH
Fold induction
4,0
3,0
2,0
1,0
0,0
*
*
NS
wt
Fbn1
wt
Fbn1
wt
Fbn1
thoracic aorta
D
2m
4m
7m
P-Smad2/3
Fold induction
4,0
3,0
2,0
1,0
0,0
*
*
NS
wt
Fbn1
wt
Fbn1
wt
Fbn1
thoracic aorta

Figure 3.2. Analysis of TGF-βs target genes expression in aorta of *Fbn1*$^{+/C1039G}$. A,C) BMP target genes analysis revealed increased Id2-3 expression at 2 months in both thoracic aorta (C) and aortic arch (A) of mutants. Moreover, Id3 induction persisted in aortic arch at 7 months, although at lower levels. B,D) Target genes analysis for TGF-β showed increased PAI-1 at 7 months only in aortic arch (B). Ctgf level was increased at 2 months in both thoracic aorta (D) and arch (B), and at 7 months only in aortic arch (B) of *Fbn1* mutants. *, P< 0,05; NS, not significant.F.in., fold induction.

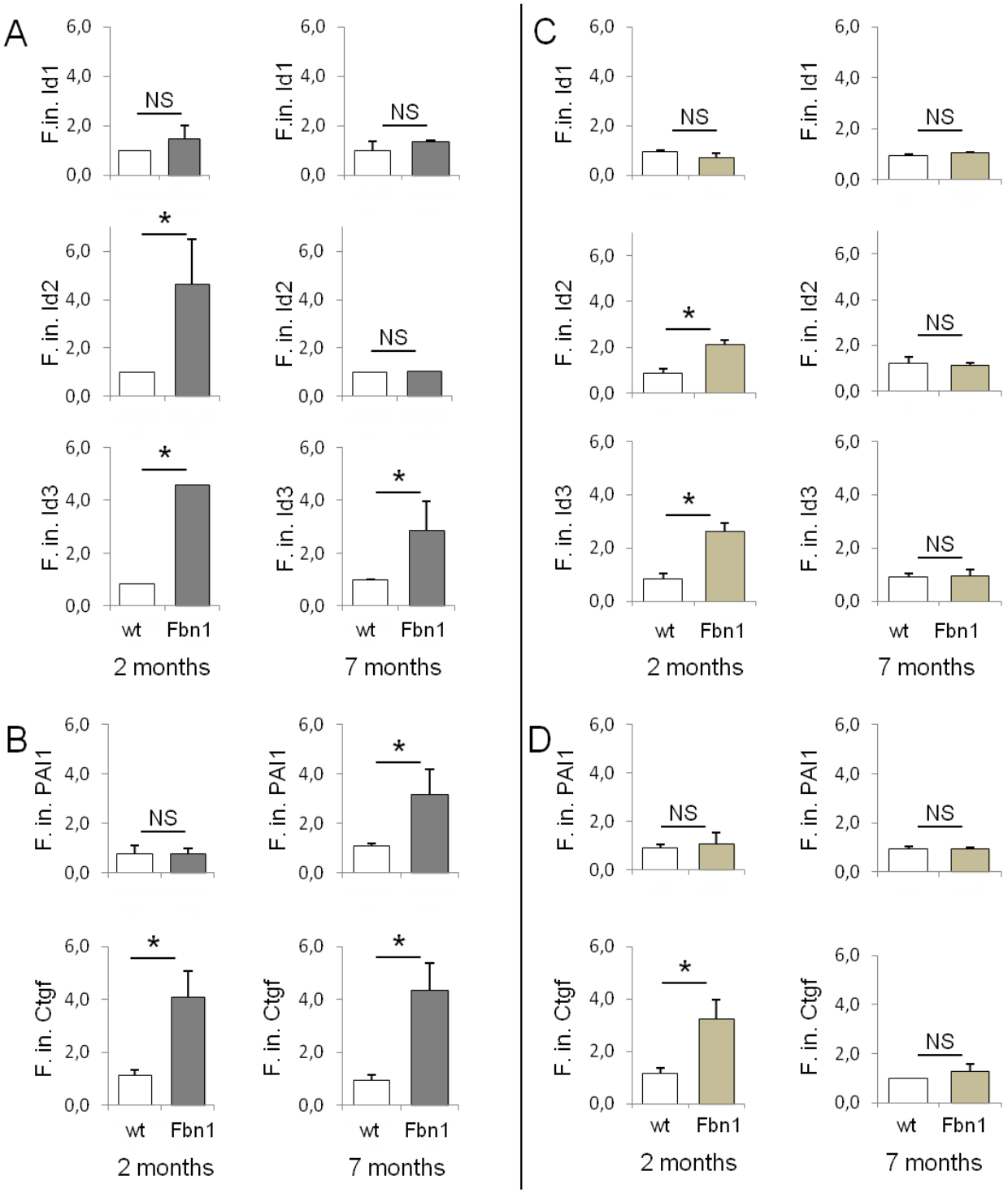
A
B
C
D
F.in. Id1
F. in. Id2
F. in. Id3
F. in. PAI1
F. in. Ctgf
6,0
4,0
2,0
0,0
NS
*
wt
Fbn1
2 months
7 months

Figure 3.3. Constructs used to generate transgenic mice with adjustable levels of TGF-β or BMP signaling. A) Schematic representation of inducible polyprotein constructs. Activity of the TRE-CMV (TC) minimal promoter can be regulated by doxycycline. caALK5 (constitutively active ALK5), Smad7 and caAlk3, Smad6 and Noggin are involved in TGF-β and BMP signaling, respectively. Expression of caALK5 and Smad7 was associated with nuclear H2BGFP; HcRed was part of the polyprotein complex used for caAlk3, Smad6 and Noggin. 2A sequence of FMD virus allowed expression of separate proteins. B-C) Schematic representation of BAC clone RP-156B9 modified by recombineering to insert rtTA cDNA downstream of the smooth myosin heavy chain promoter (*Smmhc*) (B). Modified BAC clone was used to generate a transgenic mouse line. Integration and integrity of transgenic BAC was checked by Southern Blot analysis (C), where bands indicated by arrows refer to DNA fragments with the same color indicated in (B). Probes used are indicated. Probe 1 (Pb 1) mapped on the rtTA sequence and was specific for the transgene; Probe 2 (Pb 2) was derived from the promoter region of the *Smmhc* gene and hybridizes with DNA fragments of different size derived from the transgene and the endogenous *Smmhc* gene. Restriction enzymes used are indicated.

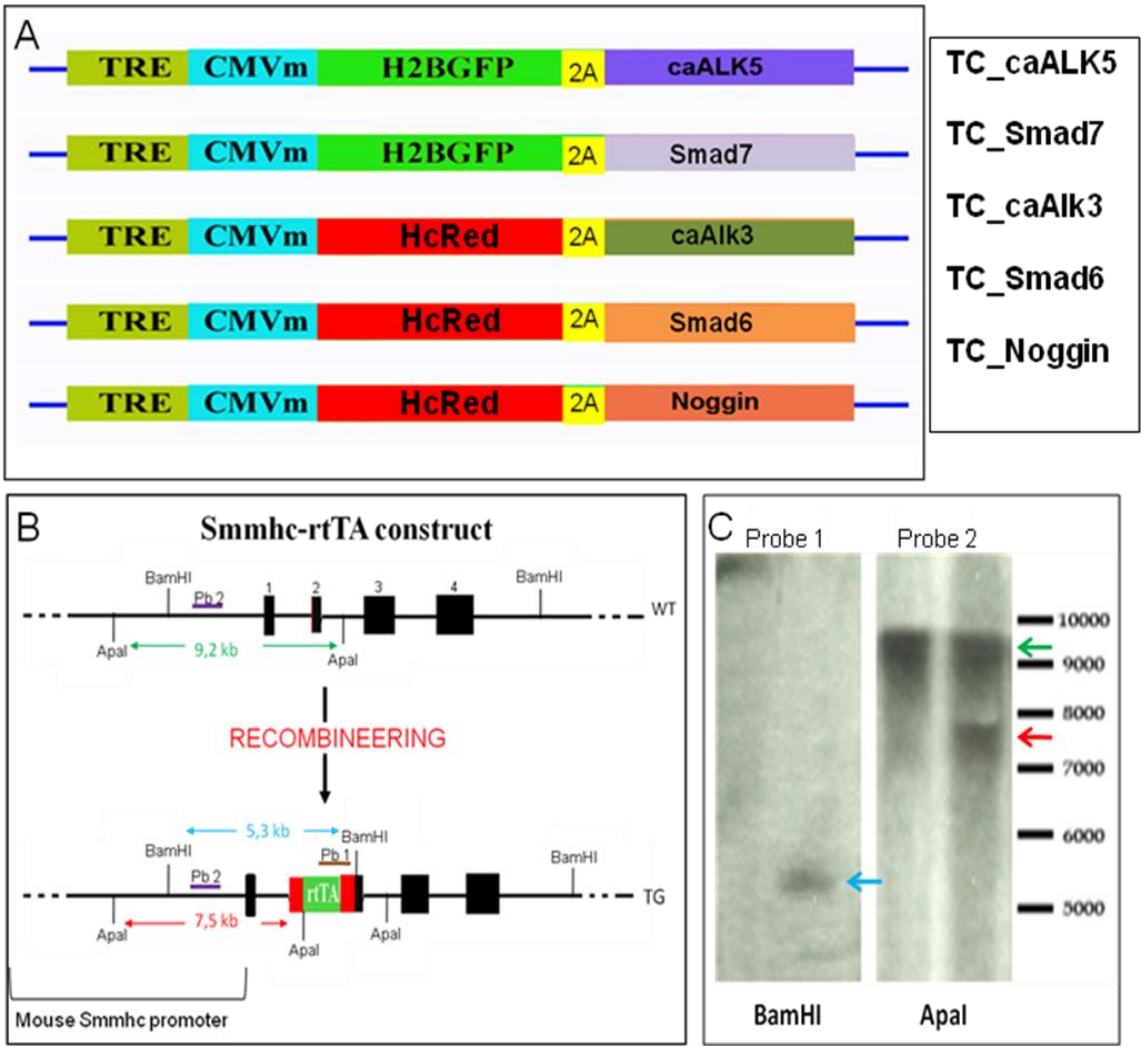
A
TRE CMVm H2BGFP 2A caALK5
TRE CMVm H2BGFP 2A Smad7
TRE CMVm HcRed 2A caAlk3
TRE CMVm HcRed 2A Smad6
TRE CMVm HcRed 2A Noggin
TC_caALK5
TC_Smad7
TC_caAlk3
TC_Smad6
TC_Noggin
B
Smmhc-rtTA construct
BamHI
Pb.2
1
2
3
4
BamHI
WT
ApaI
9,2 kb
ApaI
RECOMBINEERING
5,3 kb
BamHI
BamHI
Pb.1
BamHI
Pb.2
rtTA
TG
ApaI
7,5 kb
ApaI
ApaI
Mouse Smmhc promoter
C
Probe 1
Probe 2
10000
9000
8000
7000
6000
5000
BamHI
ApaI

Figure 3.4. Expression of cDNA for activation or inhibition of signaling. A-D) Polyprotein vectors were co-transfected in HEK293T cells with pTet-ON plasmid, that express rtTA, and reporter plasmid for luciferase assay for TGF-β, pCAGA_lux, or BMP signaling, pId1_lux. After transfection cells were treated with doxycycline 1µg/ml for 24hs. Increased TGF-β signaling was detected with expression of caALK5 only after treatment with doxycycline and in presence of rtTA (A). Inhibition of TGF-β signaling was obtained with Smad7 induction (B); instead reduction of BMP activity was reached with Smad6 (C) and Noggin (D). Expression of caAlk3 and BMP signaling activation was checked by Western Blot analysis, measuring level of phosphorylation of Smad1/5/8 (E). To note that, in all transfection, the expected activation/inhibition of growth factors signaling was observed only in presence of both rtTA and doxycycline (yellow boxes in tables). F-I) All polyprotein constructs expressed also reporter fluorescent protein. Nuclear H2BGFP was expressed by TC_caALK5 and TC_Smad7 (G), while cytoplasmic HcRed was found with plasmids TC_caAlk3, TC_Smad6 and TC_Noggin (I). +, plasmid transfected; -, plasmid not transfected; ++, double concentration of transfected plasmid.

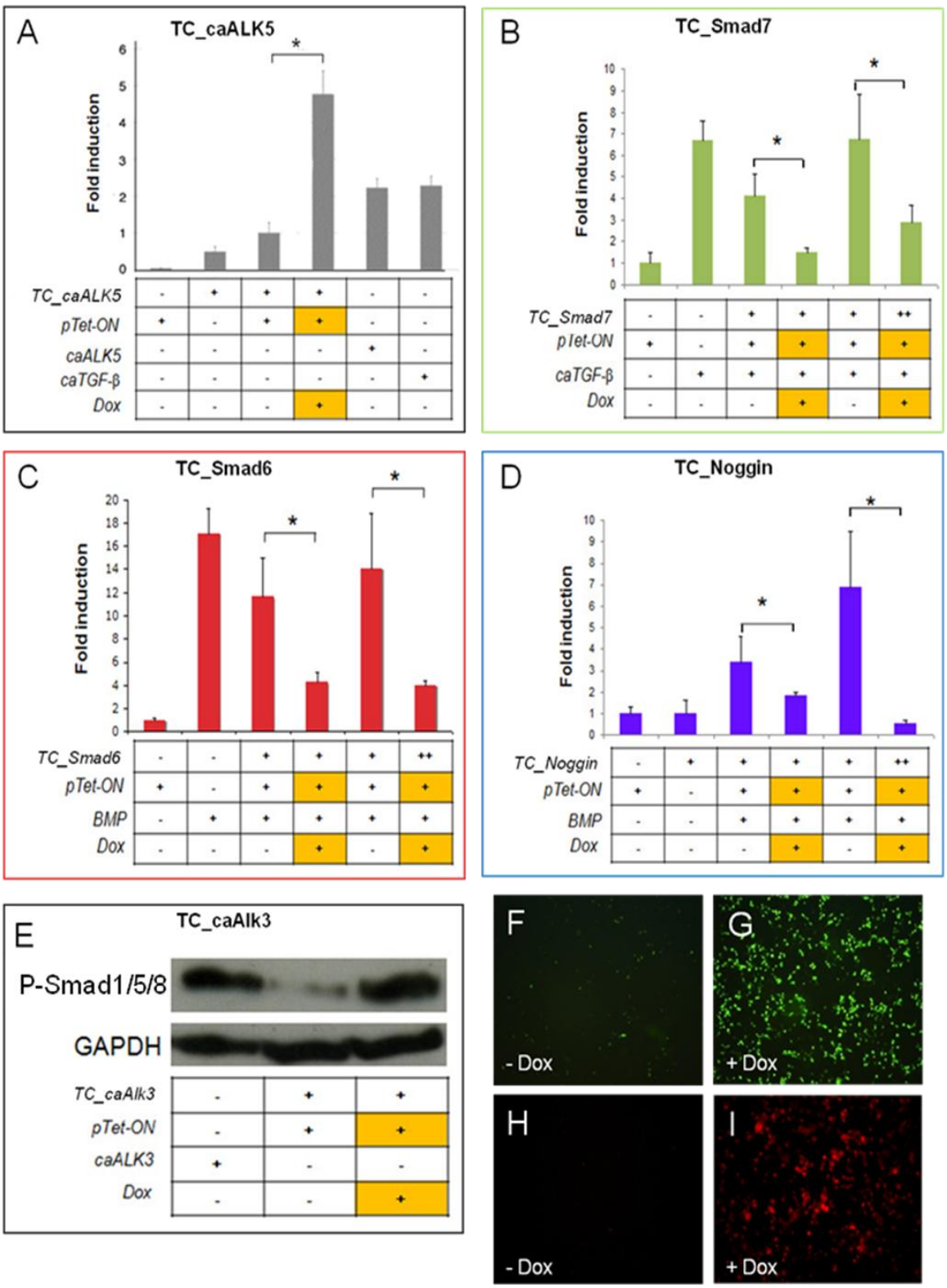
A
TC_caALK5
Fold induction
TC_caALK5
pTet-ON
caALK5
caTGF-β
Dox
B
TC_Smad7
Fold induction
TC_Smad7
pTet-ON
caTGF-β
Dox
C
TC_Smad6
Fold induction
TC_Smad6
pTet-ON
BMP
Dox
D
TC_Noggin
Fold induction
TC_Noggin
pTet-ON
BMP
Dox
E
TC_caAlk3
P-Smad1/5/8
GAPDH
TC_caAlk3
pTet-ON
caALK3
Dox
F
- Dox
G
+ Dox
H
- Dox
I
+ Dox

Figure 3.5. Characterization of the designed inducible transgenic system *in vitro* and *in vivo*. A) Cultured VSMCs from *Smmhc*-rtTA;TC_caAlk3 mice were treated with increasing doxycycline concentration for 48hs in DMEM-20% FBS. RT-PCR analysis revealed transgene induction at 100 µg/ml doxycycline concentration. B) Id expression analysis by RT-PCR showed higher level in VSMCs treated with 100 µg/ml doxycycline for all isoforms (fold induction: Id1= 2,8; Id2= 2,5; Id3= 2; fold induction compared to untreated VSMCs). C) Transgene induction in aorta of *Smmhc*-rtTA;TC_caAlk3 after 60 days of treatment with 1mg/ml in drinking water. Double transgenic mice n°34 and n°26 showed different transgene induction (4,5 and 18,12 fold respectively) compared to untreated animal. D) RT-PCR analysis of Id isoforms revealed correspondence between transgene induction and Id2 expression (fold induction: n°34, Id2= 1,76; n°26, Id2= 3,33). E) RT-PCR analysis of Noggin transgene expression level in aorta of *Smmhc*-rtTA;TC_Noggin mice treated with 10mg/ml doxycycline in drinking water for 15 days.

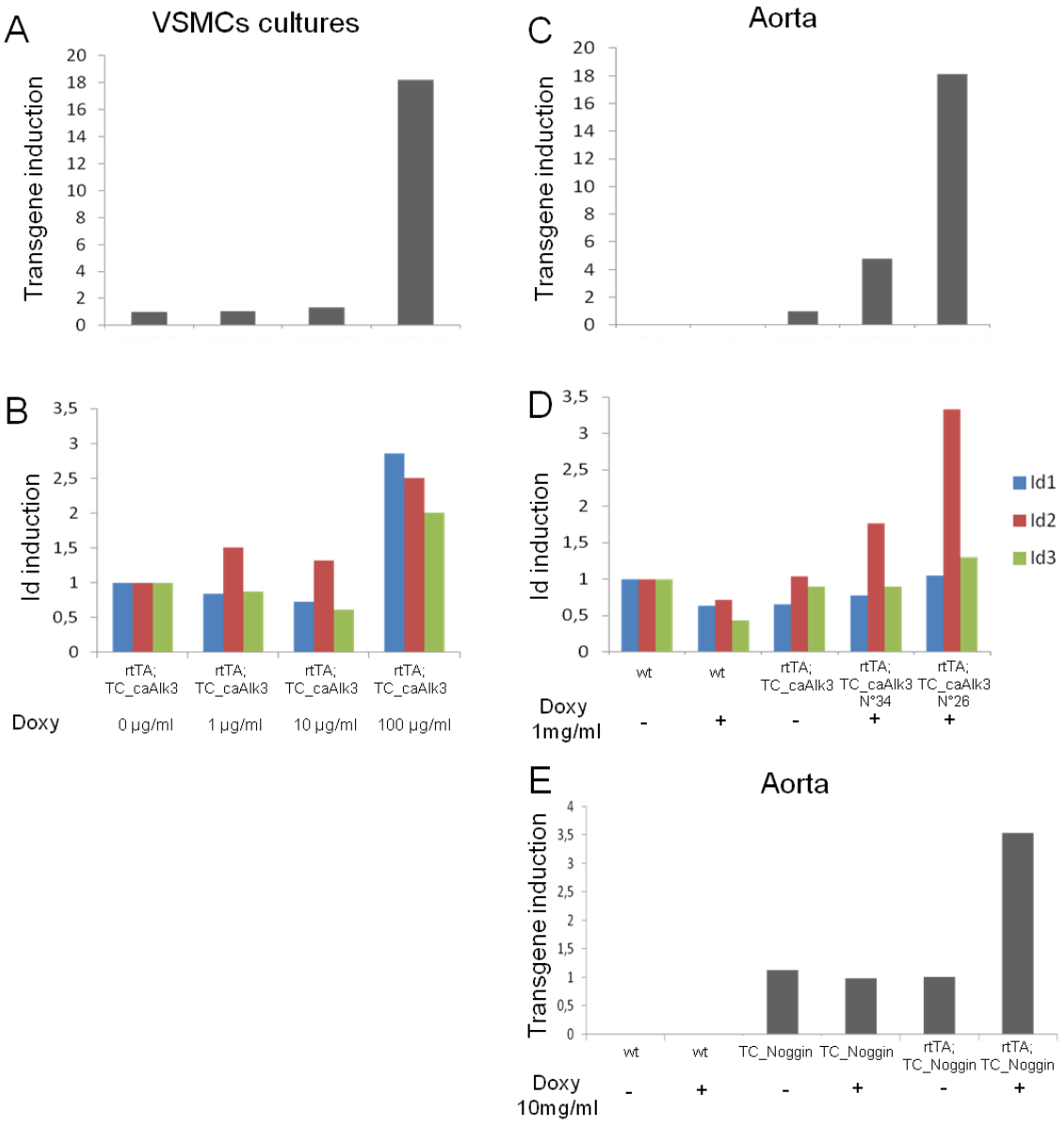
A
VSMCs cultures
Transgene induction
20
18
16
14
12
10
8
6
4
2
0
B
Id induction
3,5
3
2,5
2
1,5
1
0,5
0
rtTA; TC_caAlk3
rtTA; TC_caAlk3
rtTA; TC_caAlk3
rtTA; TC_caAlk3
Doxy
0 µg/ml
1 µg/ml
10 µg/ml
100 µg/ml
C
Aorta
Transgene induction
D
Id induction
wt
wt
rtTA; TC_caAlk3
rtTA; TC_caAlk3 N°34
rtTA; TC_caAlk3 N°26
Doxy 1mg/ml
-
+
-
+
+
Id1
Id2
Id3
E
Aorta
Transgene induction
wt
wt
TC_Noggin
TC_Noggin
rtTA; TC_Noggin
rtTA; TC_Noggin
Doxy 10mg/ml
-
+
-
+
-
+

Figure 3.6. Conditional inactivation of *Smad4* in aorta of *Smmhc*-CreER^{T2};*Smad4*$^{f/f}$ mice. A) Schematic representation of the conditional inducible system used to inactive *Smad4* in VSMCs of adult mice. The *Smmhc* promoter drives CreER^{T2} expression specifically in smooth muscle; tamoxifen treatment induces migration of the recombinase into the nucleus and excision of *Smad4* exon 8 and exon 9 flanked by the *LoxP* sequence. B) Western Blot assay showed reduction of more than 75% of Smad4 expression in aorta of *Smmhc*-CreER^{T2};*Smad4*$^{f/f}$ mice after 10 days of treatment with tamoxifen. C-D) Smad4 immunofluorescence staining of aorta sections from *Smmhc*-CreER^{T2};*Smad4*$^{f/f}$ not treated (C) and treated (D) with tamoxifen. In treated mice (D) signal (red) was lacking in the media, but persisted under the endothelium (arrows). Elastic lamellae appeared green because of autofluorescence. Images were acquired with confocal microscope. Bar, 10 µm. m, media; lu, lumen; arrows, endothelial layer.

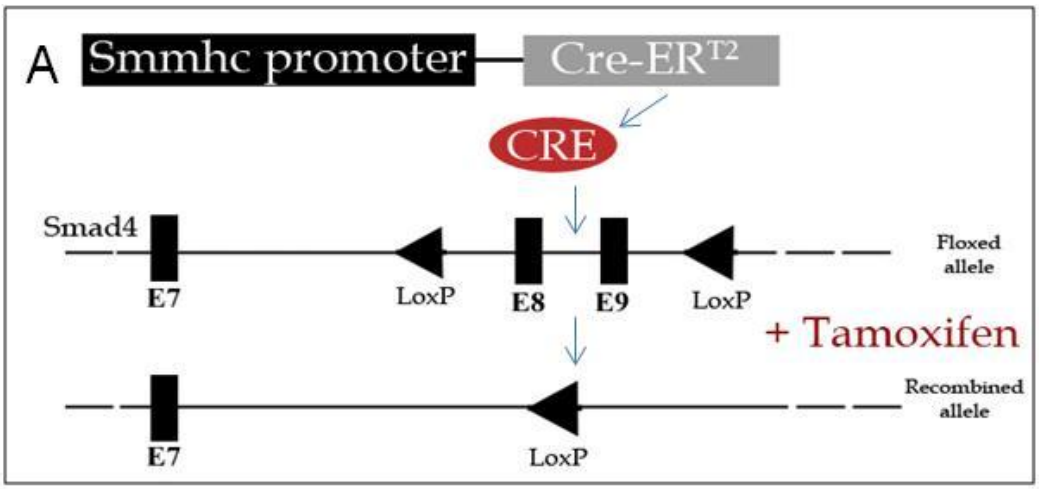
A
Smmhc promoter
Cre-ER^{T2}
CRE
Smad4
E7
LoxP
E8
E9
LoxP
Floxed allele
+ Tamoxifen
Recombined allele
E7
LoxP

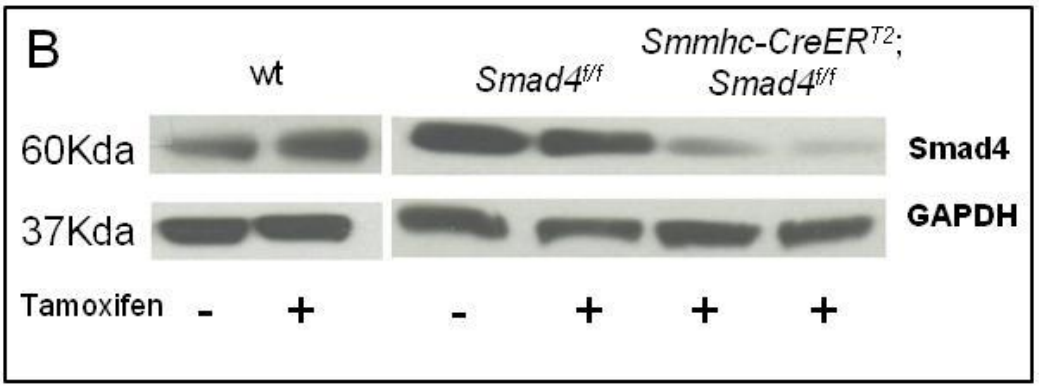
B
wt
Smad4$^{f/f}$
Smmhc-CreER^{T2}; Smad4$^{f/f}$
60Kda
37Kda
Smad4
GAPDH
Tamoxifen - + - + + +

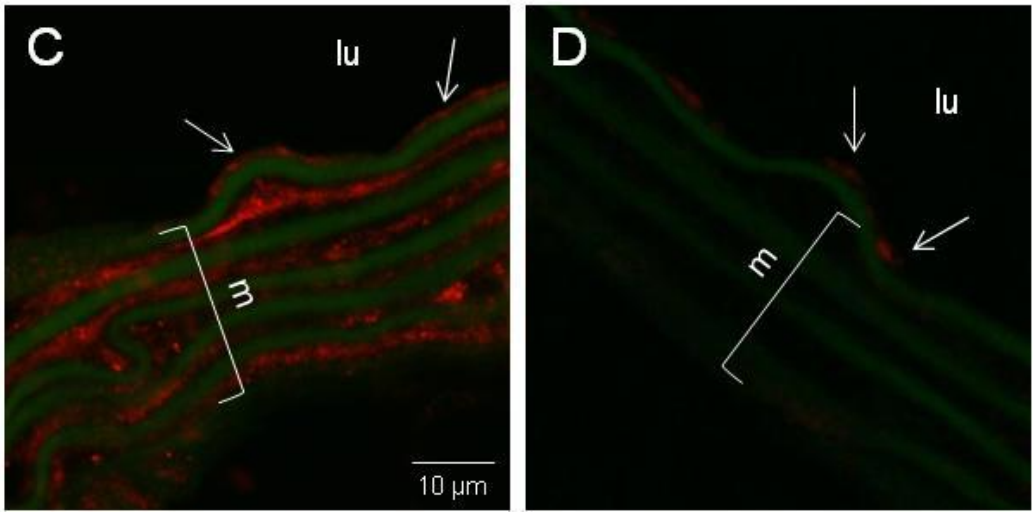
C
lu
m
10 µm
D
lu
m

Figure 3.7. Analysis of effects of *Smad4* inactivation in aorta of *Smmhc*-CreER^{T2};*Smad4*$^{f/f}$ mice. A-F) Aortic sections of wt (A,D) and *Smmhc*-CreER^{T2};*Smad4*$^{f/f}$ after 9 weeks (B,E) and 5 months (C,F) from start of tamoxifen treatment. At 9 weeks aortic arch section showed internal elastic lamellae ruptures (E, red arrow) that were more frequent at 5 months (F, red arrow). Bar, 50 µm. G) Moreover, an increase of internal elastic lamellae circumference was apparent at 5 months from treatment, suggesting aortic dilatation after *Smad4* inactivation. ***, P < 0,001. H) Survival curve of *Smmhc*-CreER^{T2};*Smad4*$^{f/f}$ mice after *Smad4* inactivation. Between 4 and 6 months from start of treatment all *Smmhc*-CreER^{T2};*Smad4*$^{f/f}$ died for aortic dissection (hemothorax). I-J,M) Tunel assay in aortic section of wt and *Smmhc*-CreER^{T2};*Smad4*$^{f/f}$ after 5 months from treatment. Count of positive cell nuclei (black arrow) showed higher number of apoptotic VSMCs in *Smad4*$^{f/f}$ aorta (M). K-L) Counter stain for nuclei with Hoechst. Bar, 10 µm.

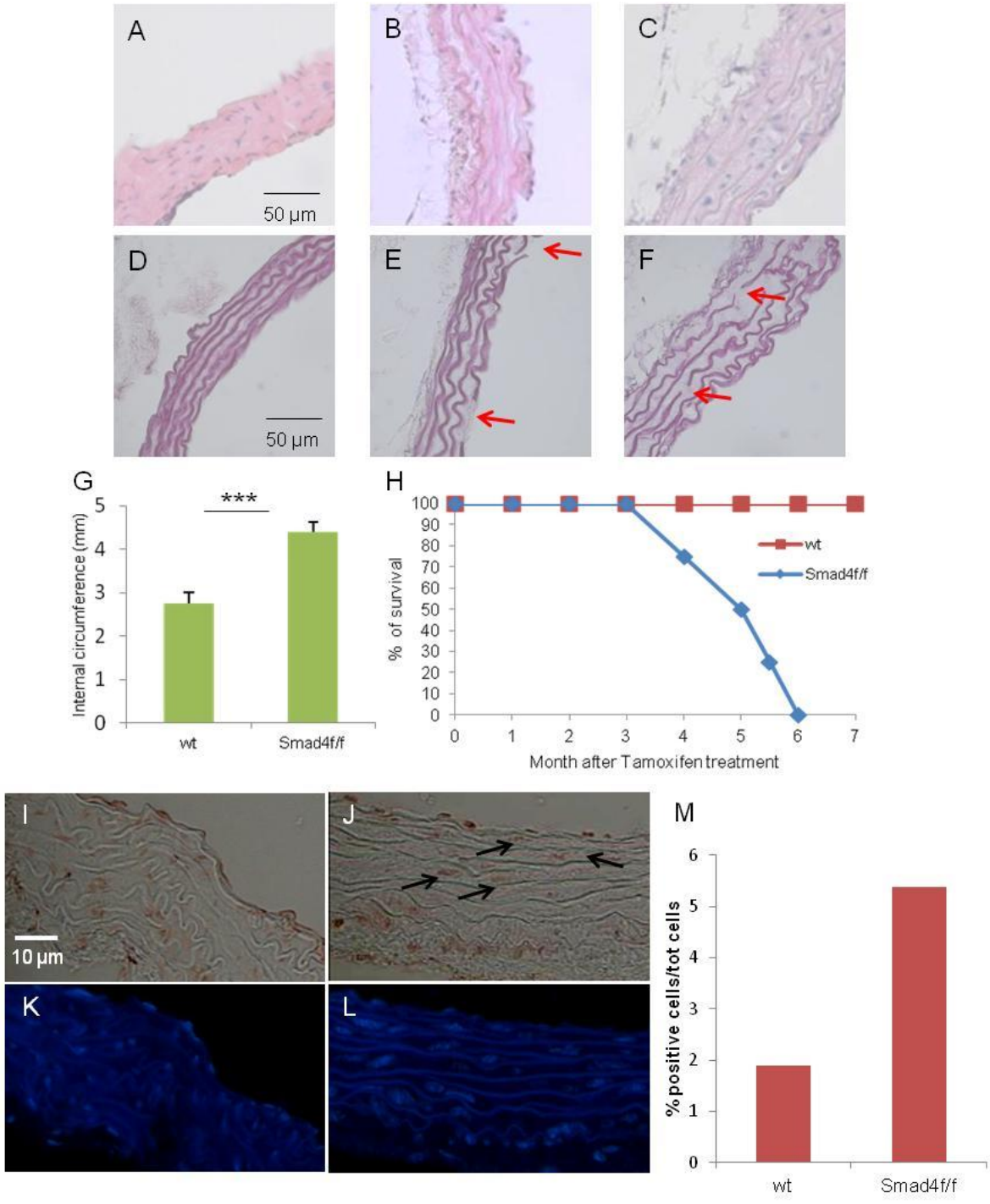
A
B
C
50 µm
D
E
F
50 µm
G
***
Internal circumference (mm)
0
1
2
3
4
5
wt
Smad4f/f
H
% of survival
100
90
80
70
60
50
40
30
20
10
0
0
1
2
3
4
5
6
7
Month after Tamoxifen treatment
wt
Smad4f/f
I
10 µm
J
K
L
M
% positive cells/tot cells
0
1
2
3
4
5
6
wt
Smad4f/f

Figure 3.8 Measurement of aortic root dilatation in *Smmhc*-CreER^{T2}; *Smad4$^{f/f}$;Fbn1$^{+/C1039G}$* and controls. A-H) Echocardiography acquisitions of aortic root of 5-month-old *Smmhc*-CreER^{T2};*Smad4$^{f/f}$;Fbn1$^{+/C1039G}$* and controls at t0 point and after 45 days from beginning of treatment with tamoxifen for 10 days. Were evident dilatations of aortic root in *Fbn1$^{+/C1039G}$* (C) and *Smmhc*-CreER^{T2};*Smad4$^{f/f}$;Fbn1$^{+/C1039G}$* (D) at t0 compared to not mutants (A-B). At t45 *Smmhc*-CreER^{T2};*Smad4$^{f/f}$;Fbn1$^{+/C1039G}$* (H) showed increased dilatation compared to *Fbn1$^{+/C1039G}$* (G), without changes in controls animal. I) Measurements of aortic root dilatation at t0, showed comparable level between wt and *Smmhc*-CreER^{T2};*Smad4$^{f/f}$*, and between *Fbn1$^{+/C1039G}$* and *Smmhc*-CreER^{T2};*Smad4$^{f/f}$;Fbn1$^{+/C1039G}$*. At t45 *Smmhc*-CreER^{T2};*Smad4$^{f/f}$;Fbn1$^{+/C1039G}$* presented significative increase in aortic root dilatation. *,P < 0,05; NS, not significant. J) Aortic root growth measurement in treated mice (t45-t0).

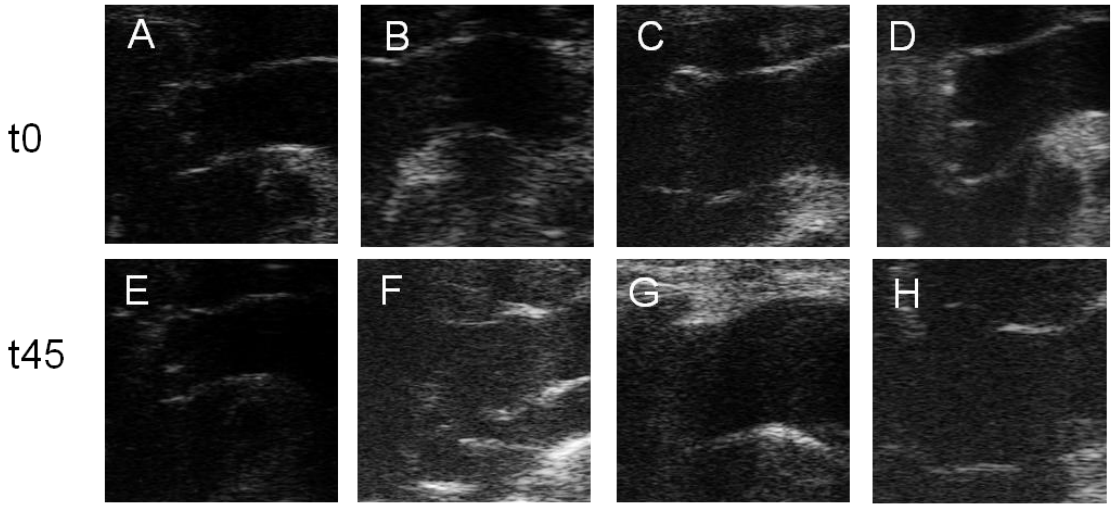
t0
t45
A
B
C
D
E
F
G
H

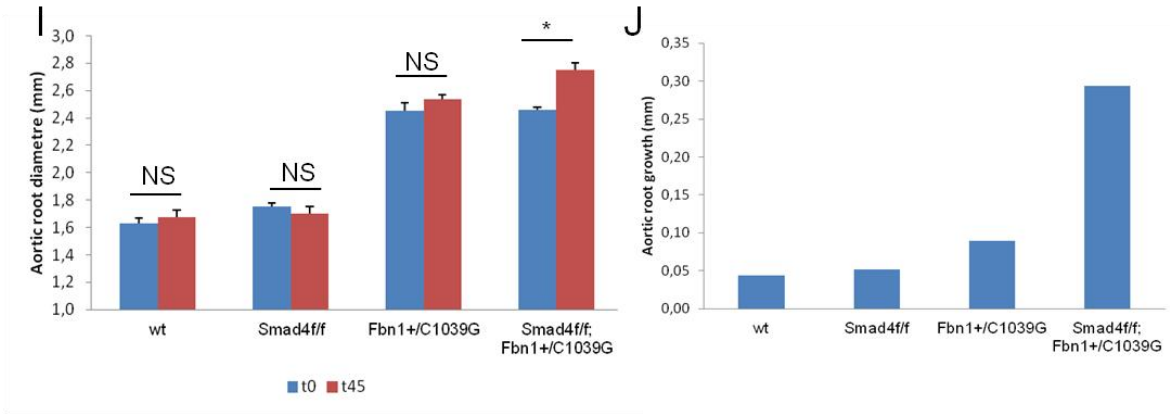
I
Aortic root diametre (mm)
3,0
2,8
2,6
2,4
2,2
2,0
1,8
1,6
1,4
1,2
1,0
NS
NS
NS
*
wt
Smad4f/f
Fbn1+/C1039G
Smad4f/f; Fbn1+/C1039G
t0
t45
J
Aortic root growth (mm)
0,35
0,30
0,25
0,20
0,15
0,10
0,05
0,00
wt
Smad4f/f
Fbn1+/C1039G
Smad4f/f; Fbn1+/C1039G

Figure 3.9. Kaplan-Meier curve of *Smmhc*-CreER^{T2};*Smad4*$^{f/f}$; *Fbn1*$^{+/C1039G}$ survival. Results were obtained with mice aged 5 months (A) and 2 months (B). In both experiments, control groups comprised 2 age-matched animals with the indicated mutation.

A

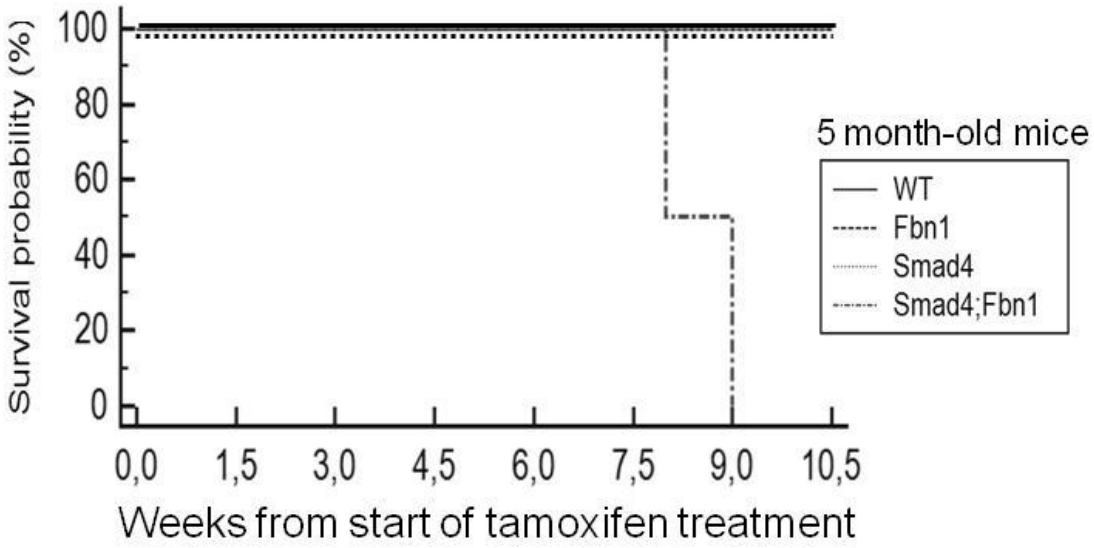
Survival probability (%)
100
80
60
40
20
0
0,0
1,5
3,0
4,5
6,0
7,5
9,0
10,5
Weeks from start of tamoxifen treatment
5 month-old mice
WT
Fbn1
Smad4
Smad4;Fbn1

B

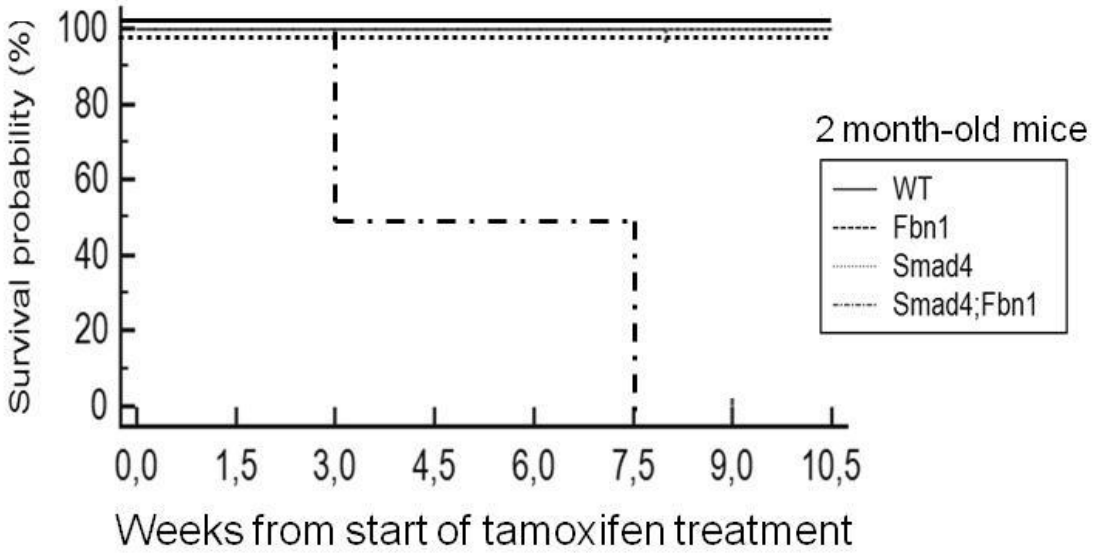
Survival probability (%)
100
80
60
40
20
0
0,0
1,5
3,0
4,5
6,0
7,5
9,0
10,5
Weeks from start of tamoxifen treatment
2 month-old mice
WT
Fbn1
Smad4
Smad4;Fbn1

Figure 3.10. Aneurysms in a *Smmhc*-CreER^{T2};*Smad4$^{f/f}$;Fbn1$^{+/C1039G}$* mouse. A-D) Macroscopic observation of aorta. The *Smmhc*-CreER^{T2}; *Smad4$^{f/f}$;Fbn1$^{+/C1039G}$* mouse, died after 53 days from start of tamoxifen treatment, showed enlarged aortic arch aneurysm (D, blue arrow) compared to age matched *Fbn1$^{+/C1039G}$* (B) and abdominal aortic aneurysm (D, red arrow) not present in controls (A-C). Magnification of thoracic aneurysm region (E-H) allowed better appreciation of the increased dilatation of aortic arch of *Smmhc*-CreER^{T2};*Smad4$^{f/f}$;Fbn1$^{+/C1039G}$* (H), with diffusion of the lesion also in ascending tract of aorta. I-L) Weigert staining. *Fbn1$^{+/C1039G}$* mice showed elastic lamellae disarray as expected (J), but increased wall damage, characterized by elastic lamellae ruptures and abnormal matrix deposition, was evident in aortic arch sections of *Smmhc*-CreER^{T2};*Smad4$^{f/f}$;Fbn1$^{+/C1039G}$* (L). *Smmhc*-CreER^{T2};*Smad4$^{f/f}$* arch was characterized by few intra-wall lamellae ruptures (K). No alterations were evident in wt control (I). M-P) Hematoxin and eosin staining of aortic root sections showed presence of inflammatory process, mainly in adventitial layer in *Smmhc*-CreER^{T2}; *Smad4$^{f/f}$;Fbn1$^{+/C1039G}$*. A, adventitia, M, media. Bar, 50 µm.

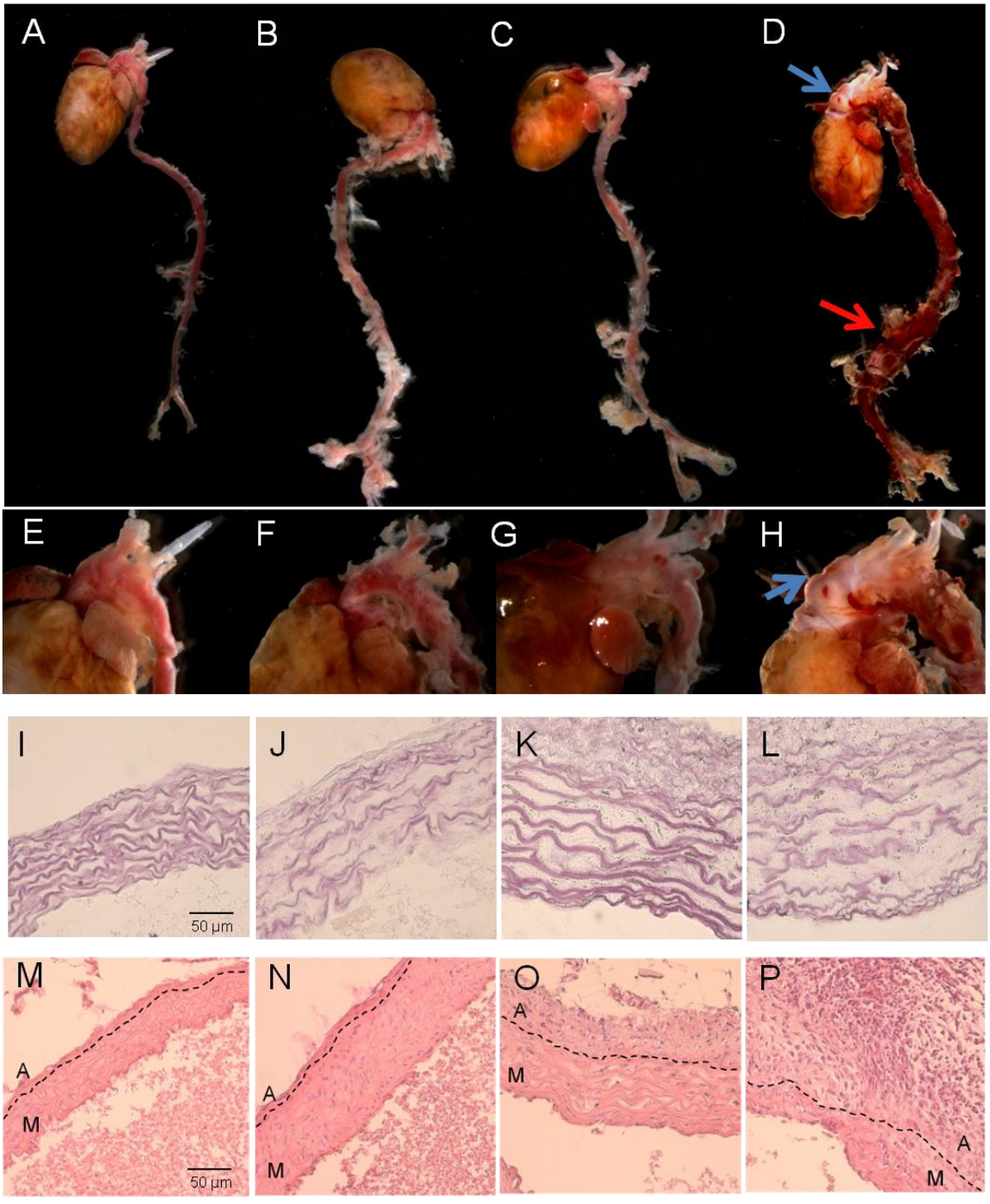
A
B
C
D
E
F
G
H
I
J
K
L
50 µm
M
A
M
50 µm
N
A
M
O
A
M
P
A
M

Figure 3.11. Appearance of abdominal aortic aneurysm (AAA) in *Smmhc*-CreER^{T2};*Smad4$^{f/f}$;Fbn1$^{+/C1039G}$* mice. A-D) Abdominal aorta region of 5-month-old mice of different genotype. Data were acquired at 2 months after start of tamoxifen treatment, when both *Smmhc*-CreER^{T2}; *Smad4$^{f/f}$;Fbn1$^{+/C1039G}$* mice died by aortic dissection. Panel D shows aorta from mouse which died for AAA rupture. E-H) Elastic lamellae staining of abdominal aortic sections showed increased wall damage in *Smmhc*-CreER^{T2};*Smad4f^{f};Fbn1$^{+/C1039G}$* (H) compared to *Fbn1$^{+/C1039G}$* age matched mice (H). Aortic wall of *Smmhc*-CreER^{T2};*Smad4$^{f/f}$;Fbn1$^{+/C1039G}$* presented more elastic lamellae ruptures and abnormal matrix deposition (F,H, dark red arrow). Moreover, an increase in aortic wall thickness was evident in *Smmhc*-CreER^{T2};*Smad4$^{f/f}$;Fbn1$^{+/C1039G}$* mice. I-L) Hematoxin and eosin staining of aortic abdominal sections of wt (I), *Fbn1$^{+/C1039G}$* (J), *Smmhc*-CreER^{T2};*Smad4$^{f/f}$* (K) and *Smmhc*-CreER^{T2};*Smad4$^{f/f}$;Fbn1$^{+/C1039G}$* (L). To note presence of inflammatory process in *Smmhc*-CreER^{T2};*Smad4$^{f/f}$; Fbn1$^{+/C1039G.}$*sections (L). Bar, 50 µm.

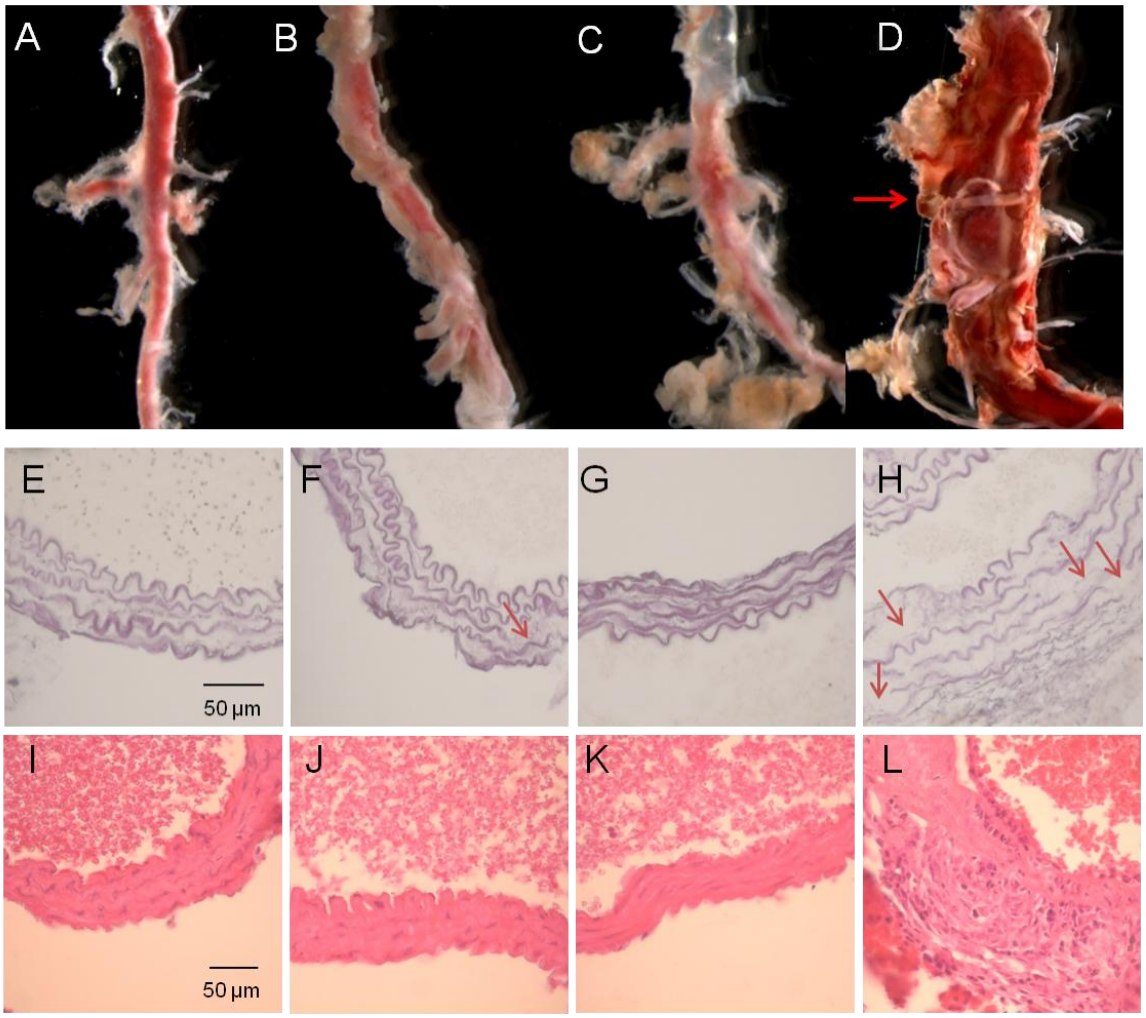
A
B
C
D
E
F
G
H
50 µm
I
J
K
L
50 µm

Figure 3.12. Increased damage, thickness wall and internal circumference in TAA and AAA of *Smmhc*-CreER^{T2};*Smad4$^{f/f}$*; *Fbn1$^{+/C1039G}$*. A-B) Measures of aortic arch (A) and abdominal (B) aortic wall thickness of two 5-month-old *Smmhc*-CreER^{T2};*Smad4$^{f/f}$;Fbn1$^{+/C1039G}$* and controls treated with tamoxifen. After inactivation of *Smad4*, *Fbn1* mutants showed increased wall thickness in abdominal aorta compared to *Fbn1$^{+/C1039G}$* age-matched (sections n=8).Measurements were taken in wall regions that not presented inflammatory infiltrate. **, P < 0,01; ***, P < 0,001; NS, not significant. C) Count of number of islands of damage, characterized by gap of elastic lamellae and deposition of extracellular matrix. *Smmhc*-CreER^{T2};*Smad4$^{f/f}$;Fbn1$^{+/C1039G}$* mice showed increased wall damage in both aortic arch and abdominal aorta (sections analyzed n= 8). D) Measurement, of internal circumference of abdominal aortic region (sections analyzed n= 6) **, P < 0,01; ***, P < 0,001; NS, not significant.

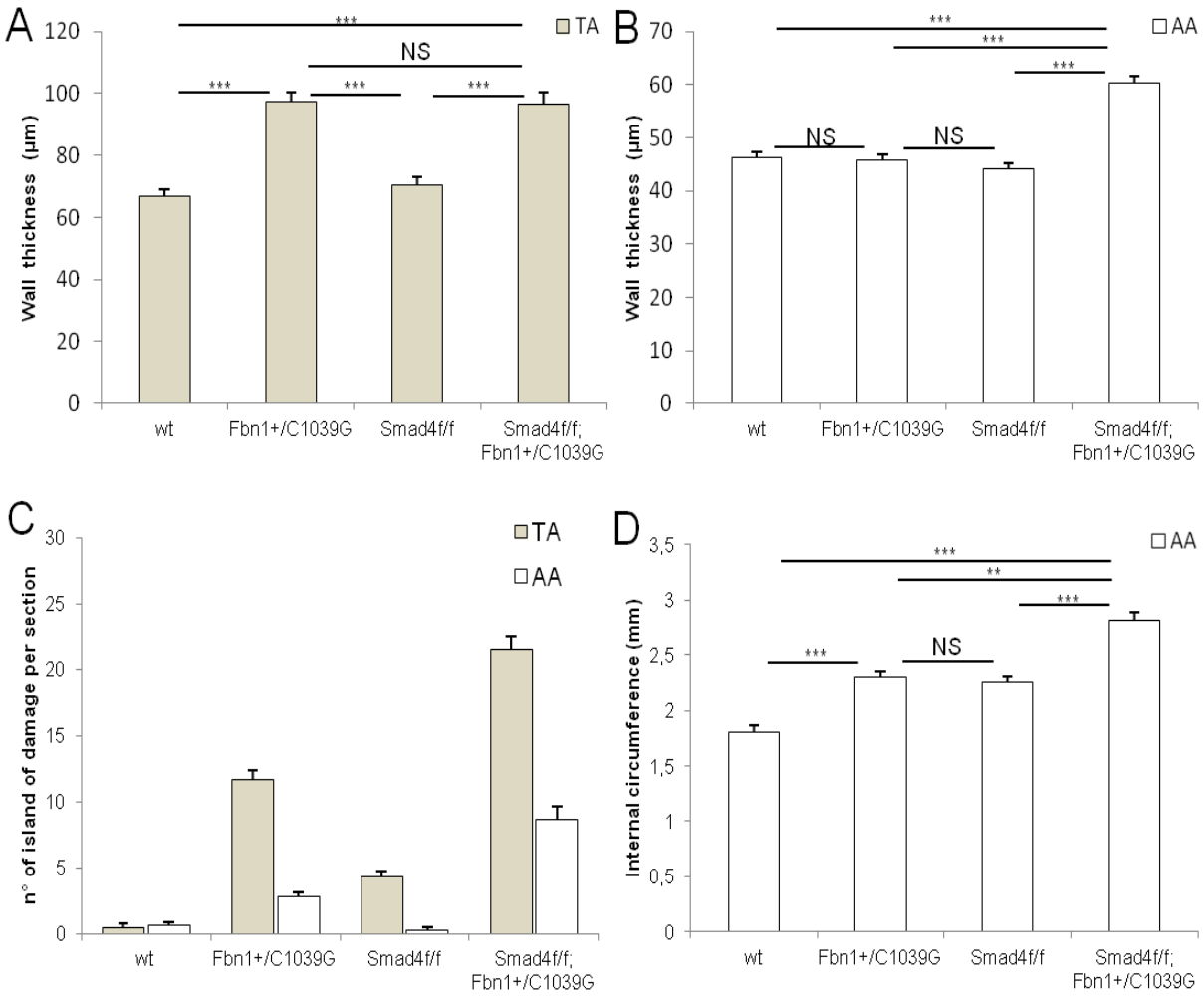
A
TA
Wall thickness (µm)
120
100
80
60
40
20
0
***
NS
***
***
***
wt
Fbn1+/C1039G
Smad4f/f
Smad4f/f; Fbn1+/C1039G
B
AA
Wall thickness (µm)
70
60
50
40
30
20
10
0
***
***
***
NS
NS
wt
Fbn1+/C1039G
Smad4f/f
Smad4f/f; Fbn1+/C1039G
C
TA
AA
n° of island of damage per section
30
25
20
15
10
5
0
wt
Fbn1+/C1039G
Smad4f/f
Smad4f/f; Fbn1+/C1039G
D
AA
Internal circumference (mm)
3,5
3
2,5
2
1,5
1
0,5
0
***
**
***
***
NS
wt
Fbn1+/C1039G
Smad4f/f
Smad4f/f; Fbn1+/C1039G

Figure 3.13 Aortic wall damage in 2-month-old *Smmhc*-CreER^{T2}; *Smad4$^{f/f}$;Fbn1$^{+/C1039G}$* after *Smad4* inactivation. Two 2-month-old *Smmhc*-CreER^{T2};*Smad4$^{f/f}$;Fbn1$^{+/C1039G}$* and controls were treated with tamoxifen for 10 days. Whole aorta of *Smmhc*-CreER^{T2};*Smad4$^{f/f}$*; *Fbn1$^{+/C1039G}$* mouse, died after 25 days from start of treatment, showed enlarge TAA (A, B blue arrow) and AAA (A, D red arrow) compared to *Fbn1$^{+/C1039G}$* (C, E). Hematoxin and eosin staining showed presence of inflammatory process in both TAA (H) and AAA sections (I). Moreover both aortic and abdominal segment presented damage of aortic wall (F,G) with ruptures of elastic lamellae and abnormal matrix deposition. Bar, 50 μm.

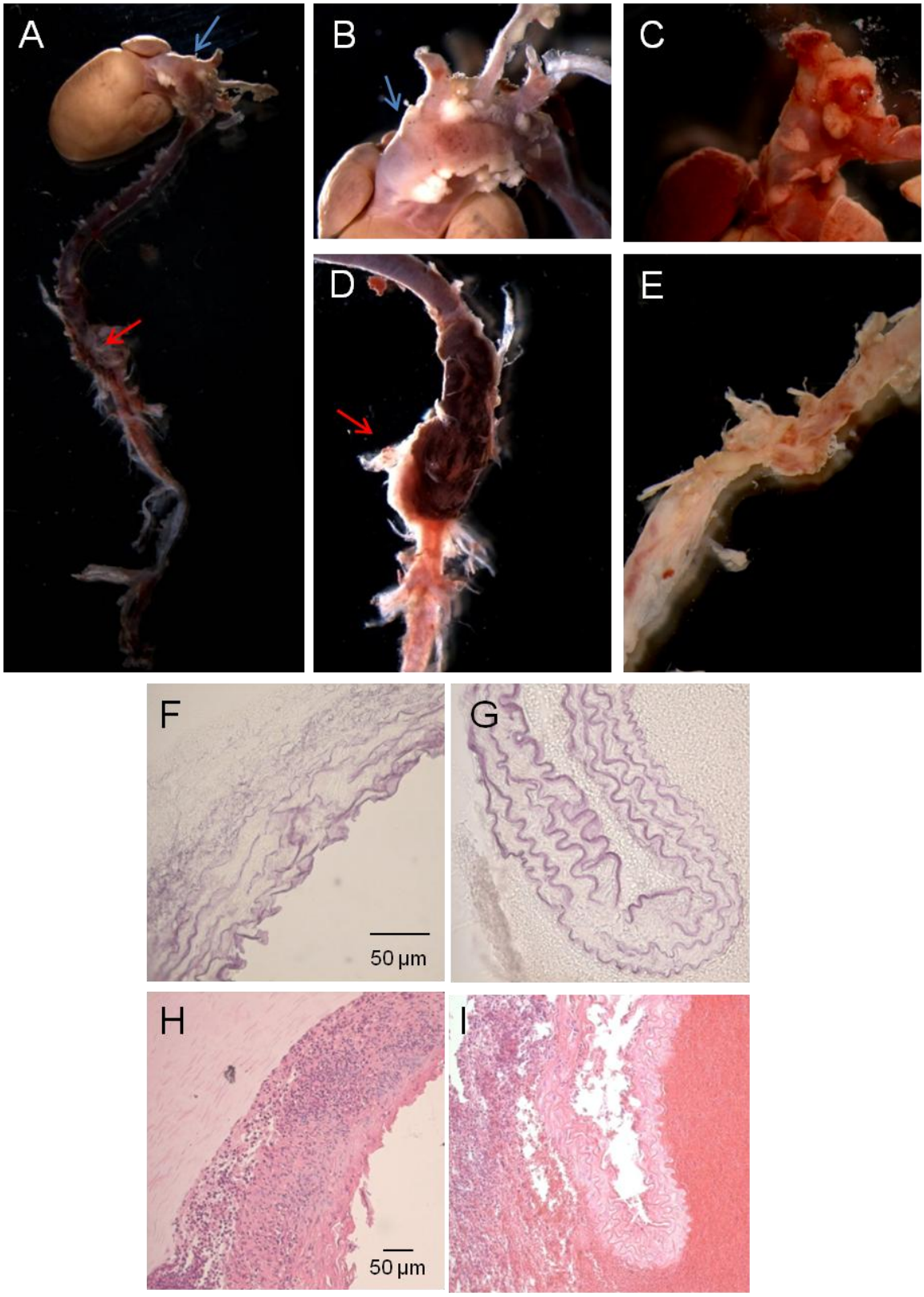
A
B
C
D
E
F
50 µm
G
H
50 µm
I

DISCUSSION

TGF-β/BMP activation levels in aorta of Fbn1$^{+/C1039G}$ mice

The research presented in this thesis is part of a larger project aiming at studying in depth the pathogenetic mechanism involved in Marfan syndrome, by means of a mouse model heterozygous for *Fbn1* mutation C1039G (*Fbn1*$^{+/C1039G}$). This model shows phenotypic and genotypic features similar to the ones observed in Marfan patients (Judge et al., 2004; Neptune et al., 2003; Holm et al., 2011). Since Fibrillin-1 is a known regulator of TGF-β/BMP availability, the starting point of this project was the analysis of molecular alterations involved in the appearance and progression of aortic root aneurysm, mainly in relation to the above mentioned growth factors. The aortic segment principally affected by aneurysms in *Fbn1*$^{+/C1039G}$ mice shows a disarray of the elastic matrix in the vessel wall, with presence of elastic lamellae ruptures and abnormal matrix deposition (Judge et al., 2004; Fig. 3.10J). The pathogenetic hypothesis currently proposed as the major cause of aneurysm manifestations involves a TGF-β signaling deregulation, possibly enhanced by Angiotensin II. Indeed different studies showed an increase of TGF-β signaling in aorta of *Fbn1* mutants measured by P-Smad2 levels (Neptune et al., 2003; Judge et al., 2004; Habashi et al., 2006; Carta et al., 2009; Holm et al., 2011).

Trying to define the role of TGF-β and BMP in aneurysm onset, we initially analyzed the activation levels of the two corresponding signaling pathways in aortas of mutant mice at different ages, separating the aortic arch from the descending aorta. Our data showed for the first time an increment in P-Smad1/5/8 level, and therefore of BMP signaling, in *Fbn1*$^{+/C1039G}$ aortas both in the arch and the descending segment. This observation is in agreement with what noted in another mouse model carrying mutations for *Fbn1* and *Fbn2* (Nistala et al., 2010). However, this activation was registered only in young animals and it was not detectable in 7-month-old mice when the mice normally show the aortic root aneurysm. Regarding the TGF-β signaling we observed an increment of P-Smad2/3 levels only at 2 and 4 months of age. Dissimilarly to what shown in 12-month-old *Fbn1*$^{+/C1039G}$ mice (Holm et al., 2011), 7-month-old mice did not revealed any difference in P-Smad2/3 level in the aortic arch (Fig.

3.1B). In addition to the low number of animals analyzed (n=2), we can suppose to have chosen an age not previously documented, in which there is a temporary reduction of TGF-β signal. Our intention is to repeat this observation, considering also older mice (12-month-old) so as to compare our results with previously published data.

In order to gain more information about TGF-β/BMP signaling activation, we performed RT-PCR analysis to assess the expression of target genes controlled by the analyzed growth factors. Among the target genes of BMP signaling, we disclosed a positive relation between Id levels and phosphorylation of Smad1/5/8 at 2 and 7 months of age, in both the aortic arch and the descending aorta. Only the Id3 level in aortic arch of 7-month-old *Fbn1*$^{+/C1039G}$ mice was increased. The Id3 increment may be due to effects of other signaling. For example, it was reported in literature that Id3 expression is influenced by Angiotensin II signaling and this can indicate a higher proliferation rate of VSMCs (Owens et al., 2011).

TGF-β target genes expression levels were not in agreement with Smad2/3 phosphorylation. Ctgf expression level partially agreed with TGF-β activation at 2 months of age in both the aortic arch and the descending aorta of *Fbn1*$^{+/C1039G}$ mice. However, in the aortic arch of 7-month-old mutants Ctgf mRNA was still increased, despite the lack of P-Smad2/3 increase. Moreover PAI-1 analysis showed an opposite trend when comparing its expression and TGF-β activation (Fig. 3.2C and Fig. 3.2D). If this finding is confirmed, increasing the number of animals analyzed (currently only 2), we could suppose that expression levels of Ctgf and PAI-1 in aortic arch of 7-month-old *Fbn1*$^{+/C1039G}$ mice may derive from effects of other signaling pathways, in addition to TGF-β, acting at the aneurysm level.

Functioning of the generated inducible expression system

In order to obtain exhaustive information about TGF-β and BMP roles on the onset and progression of thoracic aortic aneurysm (TAA), we used transgenic mice in which it was possible to modulate the activity of these two growth factors. The first transgenic system was generated in our laboratory with the objective to

easily manipulate the specific growth factor signaling. Features of this system were: i) inducibility at different ages and ii) reversibility. Using the Tet-On inducible expression methods for mammal cells and a BAC clone covering *Smmhc* gene, we generated transgenic mice in which the reverse tetracycline transactivator (rtTA) controls the expression of other transgenes, under a TRE-CMV minimal promoter, only in smooth muscle cells and after doxycycline treatment. The characterization of the system was performed only in two independent transgenic lines, in which the constitutively active BMP receptor I caAlk3 (TC_caAlk3 line) or the BMP inhibitor Noggin (TC_Noggin line) were modulated. The results showed that the inducible system works, both *in vitro* in VSMCs (TC_caAlk3) and *in vivo* in aorta (TC_Alk3 and TC_Noggin). The activation of the inducible system seems to depend, both *in vitro* and *in vivo*, on doxycycline dosage and on the length of the treatment. To better define induction capacity of the system we are going to perform time-course and dose-response studies, including in the analysis also the other transgenic lines available, TC_caALK5, TC_Smad6 and TC_Smad7. Another important result on the efficacy of the inducible system is the correlation between caAlk3 expression and target gene induction both in VSMCs and partially in aorta. Indeed these findings suggest the ability of system used to modulate the activation of BMP pathways. The lack of results about Id regulation in TC_Noggin line is, in our opinion, dependent on the difficulty in registering a reduction, instead of an induction, of basal level of these genes. More information could be obtained from *Fbn1*$^{+/C1039G}$ mice that showed higher Ids expression level compared to controls (Fig. 3.2A). We can conclude that i) a more extensive characterization of the lines is needed, but ii) the inducible system generated is adequate to modulate TGF-β and BMP signaling, both in wt and *Fbn1* mutant background. Indeed the final aim is to study the effects on the onset of vascular alteration, such as aneurysm, following the inhibition or activation of the two signaling pathways.

Effects of Smad4 inactivation in VSMCs in adult mice

The second approach used to modulate TGF-β/BMP signaling in adult mice takes advantage of an inducible recombinase CreER^{T2}, expressed under

Smmhc promoter, to inactivate *Smad4*$^{f/f}$ gene only in smooth muscle cells. Following the activation of CreER^{T2} with tamoxifen treatment of the mice, the level of *Smad4* expression in aorta decreased more than 75% after 10 days from the beginning of administration of the drug. We can suppose that the reduction of Smad4 protein is higher than that we recorded, if we consider that the inactivation was specific for smooth muscle cells and that endothelial *Smad4* expression was not affected. After 9 weeks from treatment, we detected elastic lamellae ruptures, in particular of the Internal Elastic Lamellae (IEL), without alteration in thickness wall or internal circumference. However inactivation of *Smad4* was associated with increased mortality for hemothorax after 5/6 months from the start of the treatment. Histological analysis of aortic arch sections showed increase damage and disarray of aortic wall. Moreover after 5 months from *Smad4* inactivation, an increase of internal circumference was measured, suggesting that aortic dilatation had occurred. These findings show that inhibition of both TGF-β and BMP signaling in VSMCs causes appearance of vessel alterations, similar to what observed in TAA. Comparable alterations were not detected in mice heterozygous for *Smad4* allele (Holm et al., 2011). Probably this discrepancy depends on a higher inhibition of *Smad4* in our mouse model compared to the one used in the cited work. Unlike thoracic aneurysm of *Fbn1*$^{+/C1039G}$ mice, in *Smad4*$^{f/f}$ mice the vessel wall exhibited fewer islands of damage, less deposition of matrix and compacter elastic fibers. However, despite these milder morphological damages, *Smad4*$^{f/f}$ alterations cause death of animals within 5 months, while *Fbn1*$^{+/C1039G}$ mice rarely die due to aortic dissection (Judge et al., 2004). Therefore our data suggest that the reduction of TGF-β/BMP activity is itself cause of aneurismal pathologies.

Based on the data available so far in literature, it is not yet clear if TGF-β has a protective or pejorative role on the onset and progression of aortic aneurysm. Although in many studies in animal models and humans, an increase of TGF-β signaling in aneurysm was reported (Habashi et al., 2006; Moltzer et al., 2011), recent works showed a worsening of the phenotype after inactivation of *Smad4*, without apparent modification of TGF-β activity (Holm et al., 2011). Holm and colleagues observed an increase of dilatation of aortic arch and death due to dissection in *Fbn1*$^{+/C1039G}$; *Smad4*$^{+/-}$ mice. Based on these results, we decided to

monitor the effects of *Smad4* inactivation in aorta of adult *Smmhc*-CreER^{T2};*Smad4*$^{f/f}$;*Fbn1*$^{+/C1039G}$ mice. After TGF-β/BMP signaling inhibition, we registered an increase of aortic dilatation at Sinus of Valsalva, and death due to dissection, as reported by Holm and colleagues. However macroscopic observation of aorta of *Smmhc*-CreER^{T2};*Smad4*$^{f/f}$;*Fbn1*$^{+/C1039G}$ mice showed appearance of abdominal aortic aneurysm (AAA), at the level of renal arteries outflow. This phenotype has never been documented so far in *Fbn1*$^{+/C1039G}$ mice. Furthermore the deaths of *Smmhc*-CreER^{T2};*Smad4*$^{f/f}$;*Fbn1*$^{+/C1039G}$ were mostly due to abdominal rather than thoracic dissection. These results induce to consider the data proposed by Wang and colleagues in a different perspective. They found a worsening of Angiotensin II-induced AAA, after suppression of TGF-β activity with neutralizing antibody, and they suggested an inhibitory effect of this growth factor on the manifestation of aneurysms (Wang et al., 2010). We found inflammatory process in the adventitial layer of altered vessel, but the impression coming from the limited observations of this thesis is that inflammation is not relevant for the structural alterations of the aortic wall induced by *Fbn1* and *Smad4* mutations, however important in accelerating the process of aneurysm dissection.

In conclusion our data only partially agree with the hypothesis that the manifestation of aneurysms in Marfan syndrome is due to increase of TGF-β signaling, and urge to investigate the following points:

1) Distinguishing between TGF-β and BMP role. Using the inducible expression system generated to modulate TFG-β/BMP signaling, we can inhibit TGF-β or BMP activity in *Fbn1*$^{+/C1039G}$ after expression of Smad7 and Smad6 respectively. At the same time, we are going to monitor manifestation and progression of aortic aneurysm in *Fbn1*$^{+/C1039G}$;*TGF-β1*$^{+/-}$, using for the first time a genetic approach, and not immunological (Habashi et al., 2006), to inhibit TGF-β signaling.
2) Verifying with new experiments if the increase of P-Smad2/3 or TGF-β target genes expression in *Fbn1* mutants correspond to real activation of TGF-β pathways. Otherwise, the lack of correlation would suggest that other signalings are involved in pathogenesis of Marfan aneurysm.

3) Testing the effects of gain or loss-of function of signaling potentially implicated in Marfan syndrome. Some indications were presented in works of Holm and colleagues and they concerned MAPK p38 and JNK. However, we have to consider also other signaling, as the ones activated by integrins.

Actually the pathogenesis of Marfan syndrome seems to be still unclear, although numerous studies had reported important information. Therefore, all hypotheses that concern the behavior of cells (i.e. alteration of mechano-transduction) and based on exhaustive experimental approaches may be considered in the study of Marfan syndrome models. This Phd thesis aims at giving a small contribution in this prospective.

REFERENCES

Agrotis, A., Kalinina, N., Bobik, A. (2005). Transforming growth facton-B, cell-signaling and cardiovascular disorders. Curr. Vasc. Pharm. 3,55-61.

Annes, J.P., Munger J.S., Rifkin D.B. (2003). Making sense of latent TGFβ activation. J. Cell Sci. 116, 217-224.

Argraves W.S., Greene L.M., Cooley M.A., and Gallagher W.M. (2003) Fibulins: physiological and disease perspectives.Embo rep. 4, 1127-1131.

Carta, L., Smaldone, S., Zilberberg, L., Loch D., Dietz, H.C., Rifkin D.B., Ramirez F. (2009). P38 MAPK is a early determinant of promiscuosus Smad2/3 signaling in the aortas of Fibrillin-1 (Fbn1)-null mice. J. Biol. Chem. 284, 5630-5636.

Chung Ada W.Y., Karen Au Yeung, George G.S. Sandor, Daniel P. Judge, Harry C. Dietz and Cornelis van Breemen (2007). Loss of Elastic Fiber Integrity and Reduction of Vascular Smooth Muscle Contraction Resulting From the Upregulated Activities of Matrix Metalloproteinase-2 and -9 in the Thoracic Aortic Aneurysm in Marfan Syndrome. Circ. Res. 101:512-522.

Cohn RD, van Erp C, Habashi JP, Soleimani AA, Klein EC, Lisi MT, Gamradt M, ap Rhys CM, Holm TM, Loeys BL, Ramirez F, Judge DP, Ward CW, Dietz HC (2007). Angiotensin II type 1 receptor blockade attenuates TGF-beta-induced failure of muscle regeneration in multiple myopathic states. Nat Med. Feb;13(2):204-10.

Curran ME, Atkinson DL, Ewart AK, Morris CA, Leppert MF, Keating MT (1993) The elastin gene is disrupted by a translocation associated with supravalvular aortic stenosis. Cell 73:159-168.

Dabovic, B., Chen, Y., Colarossi, C., Zambuto, L., Obata, H., Rifkin, D.B. (2002). Bone defects in laten TGF-β binding proteine (Ltbp)-3 null mice; a role for Ltbp in TGF-β presentation. J. End. 175, 129-141.

Donelly M.L.L., Hughes L.E., Luke G., Mendoza H., ten Dam E. (2001) The 'cleavage' activities of foot-and-mouth disease virus 2A site-directed mutants and naturally occurring '2A-like' sequences. J.Gen.Vir.82, 1027–1041.

Greenlee TK, Ross R, Hartman JL (1966). The fine structure of elastic fibers. J Cell Biol 30:59-71.

Faury G, Pezet M, Knutsen RH, Boyle WA, Heximer SP, McLean SE, Minkes RK, Blumer KJ, Kovacs A, Kelly DP, Li DY, Starcher B, Mecham RP. (2003).Developmental adaptation of the mouse cardiovascular system to elastin haploinsufficiency. J Clin Invest 112:1419-1428.

Holm TM, Habashi JP, Doyle JJ, Bedja D, Chen Y, van Erp C, Lindsay ME, Kim D, Schoenhoff F, Cohn RD, Loeys BL, Thomas CJ, Patnaik S, Marugan JJ, Judge DP, Dietz HC.(2011) Noncanonical TGFβ signaling contributes to aortic aneurysm progression in Marfan syndrome mice. Science. 332:358-61.

Habashi Jennifer P., Daniel P. Judge, Tammy M. Holm, Ronald D. Cohn, Bart L. Loeys, Timothy K. Cooper, Loretha Myers, Erin C. Klein, Guosheng Liu, Carla Calvi,

Megan Podowski, Enid R. Neptune, Marc K. Halushka, Djahida Bedja, Kathleen Gabrielson, Daniel B. Rifkin, Luca Carta, Francesco Ramirez, David L. Hus, and Harry C. Dietz (2006) Losartan, an AT1 Antagonist, Prevents Aortic Aneurysm in a Mouse Model of Marfan Syndrome. Science. 312: 117–121.

Habashi JP, Doyle JJ, Holm TM, Aziz H, Schoenhoff F, Bedja D, Chen Y, Modiri AN, Judge DP, Dietz HC.(2011) Angiotensin II type 2 receptor signaling attenuates aortic aneurysm in mice through ERK antagonism. Science. 332:361-365.

Judge DP, Biery NJ, Keene DR, Geubtner J, Myers L, Huso DL, Sakai LY, Dietz HC. (2004). Evidence for a critical contribution of haploinsufficiency in the complex pathogenesis of Marfan syndrome. J. Clin Invest.114: 172-181.

Judge, D.P. And Dietz, H.C., (2005). Marfan's syndrome. NIH-PA 366: 1965-1976.

Karnik SK, Brooke BS, Bayes-Genis A, Sorensen L, Wythe JD, Schwartz RS, Keating MT, Li DY (2003). A critical role for elastin signaling in vascular morphogenesis and disease. Development 130:411-423.

Laird PW, Zijderveld A, Linders K, Rudnicki MA, Jaenisch R, Berns A (1991) Simplified mammalian DNA isolation procedure. Nucleic Acids Res 19:4293.

Li DY, Brooke B, Davis EC, Mecham RP, Sorensen LK, Boak BB, Eichwald E, Keating MT (1998). Elastin is an essential determinant of arterial morphogenesis. Nature 393:276-280.

Lindasy Mark E. and Dietz Harry C. (2011) Lessons on the pathogenesis of aneurysm from heretable conditions. Nature 473: 308-316.

Loeys BL, Schwarze U, Holm T, Callewaert BL, Thomas GH, Pannu H, De Backer JF, Oswald GL, Symoens S, Manouvrier S, Roberts AE, Faravelli F, Greco MA, Pyeritz RE, Milewicz DM, Coucke PJ, Cameron DE, Braverman AC, Byers PH, De Paepe AM, Dietz HC. (2006). Aneurysm syndromes caused by mutations in the TGF beta receptor. N. Engl. J. Med. 355:788-798.

Matt P, Schoenhoff F, Habashi J, Holm T, Van Erp C, Loch D, Carlson OD, Griswold BF, Fu Q, De Backer J, Loeys B, Huso DL, McDonnell NB, Van Eyk JE, Dietz HC; GenTAC Consortium (2009). Circulating transforming growth factor-beta in Marfan syndrome. Circulation. 11;120(6):526-532.

Mazzieri, R., Jurukovski, V., Obata, H., Sung, J., Platt, A., Annes, E., Karaman-Jurukovska, N., Gleizes, PE., Rifkin, D.B. (2005). Expression of truncated latent TGF-β binding protein modulates TGF-β signaling. J. Cell. Sci. 118: 2177-2187.

Miyazono K., Maeda S., Imamura T. (2005). BMP receptor siganling: transcriptional targets, regulation of signal and signaling cross-talk. Cytokine Growth Factor Rev. 16(3):251-263.

Mizuguchi T, Collod-Beroud G, Akiyama T, Abifadel M, Harada N, Morisaki T, Allard D, Varret M, Claustres M, Morisaki H, Ihara M,Kinoshita A, Yoshiura K , Junien C, Kajii T, Jondeau G, Ohta T, Kishino T, Furukawa Y, Nakamura Y, Niikawa N, Boileau C,Matsumoto N. (2004).Heterozygous TGFBR2 mutations in Marfan syndrome. Nature Gen. 36: 855-860.

Moltzer E, te Riet L, Swagemakers SM, van Heijningen PM, Vermeij M, van Veghel R, Bouhuizen AM, van Esch JH, Lankhorst S,Ramnath NW, de Waard MC, Duncker DJ, van der Spek PJ, Rouwet EV, Danser AH, Essers J.(2011). Imparied vascular contractility and aortic wall degeneration in fibulin-4 deficient mice: effect of angiotensin II type 1 (AT1) receptor blockade. PlosOne. 6: e23411.

Nagy,A., Gertsenstein,A., Vintersten, K., Behringer, R., (2003). Manipulating the MouseEmbryo: A LaboratoryManual. Cold Spring Harbor Laboratory Press, Cold Spring Harbor, NY.

Nataatmadja M, West J, West M. (2006) Overexpression of transforming growth factor-beta is associated with increased hyaluronan content and impairment of repair in Marfan syndrome aortic aneurysm. Circulation. 114: 371-377.

Neptune, E.R., Frischmeyer, P.A., Arking, D.E., Myers, L., Bunton, T.E., Gayraud, B., Ramirez, F., Sakai, L.Y., and Dietz, H.C. (2003). Dysregulation of TGF-beta activation contributes to pathogenesis in Marfan syndrome. Nat. Genet. 33: 407–411.

Owens III A.P., Subramanian V., Moorleghen J.J., Guo Z., McNamara C.A., Cassis L.A. and Daugherty A. (2010). Angiotensin II induces a region-specific Hyperplasia of the ascending aorta through regulation of inhibitor of differentiation 3. Cric. Res. 106: 611-619.

Ramirez, F., Rifkin, D.B. (2009). Extracellular microfibrilis: contextual plattforms for TGFβ and BMP signaling. Curr. Op. Cell Biol. 21: 616-622.

Ramirez, F., Sakai, L.Y. (2009). Biogenesis and function of fibrillin assemblies. Cell Tissue Res. 339:71-82.

Rajewsky K, Gu H, Kühn R, Betz UA, Müller W, Roes J, Schwenk F (1996). Conditional gene targeting. J Clin Invest 98:600-603.

Sakai LY, Keene DR, Engvall E. (1986) Fibrillin, a new 350-kD glycoprotein, is a component of extracellular microfibrils. J Cell Biol 103:2499-2509.

Sambrook J, Fritsch EF, Maniatis T. Molecular cloning-A laboratory manual-Second edition. Cold Spring Harbor Laboratory Press, 1989.

Sauer B, Henderson N (1988). Site-specific DNA recombination in mammalian cells by the Cre recombinase of bacteriophage P1. Proc Natl Acad Sci USA 85:5166-5170.

Sengle G., Charbonneau N.L., Ono R.N., Sasaki T., Alvarez J., Keene D.R., Ba¨chinger H.P., and Sakai L.Y. (2008).Targeting of Bone Morphogenetic Protein Growth Factor Complexes to Fibrillin. J. Biol. Chem. 283: 13874-13888.

Sieber, C., Kopf, J., Hiepen, C., Knaus, P. (2009). Recent advances in BMP receptor signaling. Cytokine Growth Factor Rev. 20:343-355.

Shi Minlong, Zhu Jianghai, Wang Rui, Chen Xing, Mi Lizhi, Walz Thomas and Springer Timothy A. (2011). Latent TGF-β structure and activation. Nature 474, 343-349.

Schrijver, I., Liu, W., Brenn, T., Furthmayr, H., and Francke, U. (1999). Cysteine substitutions in epidermal growth factor-like domains of fibrillin-1: distinct effects on biochemical and clinical phenotypes. *Am. J. Hum. Genet.* 65:1007–1020.

Sternberg N (1981). Bacteriophage P1 site-specific recombination. III. Strand exchange during recombination at lox sites. J Mol Biol 150:603-608.

Sternberg N, Hamilton D (1981). Bacteriophage P1 site-specific recombination. I. Recombination between loxP sites. J Mol Biol 150:467-486.

Syyong HT, Chung AWY, Yang HHC and Breemen C van (2009). Dysfunction of endothelial and smooth muscle cells in small arteries of a mouse model of Marfan syndrome. Br. J. Pharm. 158: 1597-1608.

Syyong HT, Chung AW, van Breemen C.(2011) Marfan syndrome decreases Ca^{2+} wave frequency and vasoconstriction in murine mesenteric resistance arteries without changing underlying mechanisms. J. Vasc.Res. 48:150-162.

Ten Dijke P. and Arthur H.M. (2007). Extracellular control of TGFbeta signalling in vascular development and disease. Nat. Rev. Mol. Cell. Biol. 8:857-869.

van de Laar IM, Oldenburg RA, Pals G, Roos-Hesselink JW, de Graaf BM, Verhagen JM, Hoedemaekers YM, Willemsen R, Severijnen LA, Venselaar H, Vriend G, Pattynama PM, Collée M, Majoor-Krakauer D, Poldermans D, Frohn-Mulder IM, Micha D,Timmermans J, Hilhorst-Hofstee Y, Bierma-Zeinstra SM, Willems PJ, Kros JM, Oei EH, Oostra BA, Wessels MW, Bertoli-Avella AM. (2011) Mutations in SMAD3 cause a syndromic form of aortic aneurysms and dissections with early-onset osteoarthritis. Nat Genet. 43:121-126.

Vehviläinen P, Hyytiäinen M, Keski-Oja J. (2009). Matrix association of latent TGF-beta binding protein-2 (LTBP-2) is dependent on fibrillin-1.J. Cell Physiol. 221: 586-593.

Velasco S, Alvarez-Muñoz P, Pericacho M, Dijke PT, Bernabéu C, López-Novoa JM, Rodríguez-Barbero A.(2008) L- and S-endoglin differentially modulate TGFbeta1 signaling mediated by ALK1 and ALK5 in L6E9 myoblasts. J Cell Sci.121:913-919.

Wang Yu, Hafid Ait-Oufella, Olivier Herbin, Philippe Bonnin, Bhama Ramkhelawon, Soraya Taleb, Jin Huang, Georges Offenstadt,2 Christophe Combadière, Laurent Rénia, Jason L. Johnson, Pierre-Louis Tharaux, Alain Tedgui, and Ziad Mallat (2010). TGF-β activity protects against inflammatory aortic aneurysm progression and complications in angiotensin II–infused mice.J.Clin.Inv 12: 403-432.

Yanagisawa H, Davis EC, Starcher BC, Ouchi T, Yanagisawa M, Richardson JA, Olson EN (2002). Fibulin-5 is an elastin-binding protein essential for elastic fibre development in vivo. Nature 415:168-171.

Yang HH Clarice, Jong Moo Kim*, Elliott Chum, Cornelis van Breemen and Ada WY Chung (2009). Long-term effects of losartan on structure and function of the thoracic aorta in a mouse model of Marfan syndrome. British J. Phar., 158: 1503–1512.

Zacchigna, L., Vecchione, C.,Notte, A., Cordenonsi, M., Dupont, S., Maretto, Silvia., Cifelli, G., Ferrari, A., Maffei, A., Fabbro, C., Braghetta, P., Marino, G., Selvetella, G., Aretini, A., Colonnese, C., Bettarini, U., Russo, G., Soligo, S., Adorno, M., Bonaldo, P., Volpin, D., Piccolo, S., Lembo, G., Bressan, G.M. (2006). Emilin1 links TGF-B maturation to blood pressure homeostasis. Cell 124: 929-942.

Zhang H, Apfelroth SD, Hu W, Davis EC, Sanguineti C, Bonadio J, Mecham RP, Ramirez F(1994). Structure and expression of fibrillin-2, a novel microfibrillar component preferentially located in elastic matrices. J Cell Biol 124:855-863.

APPENDIX

Conditional inducible system used to inactivation of Smad4 in VSMCs of adult mice

The field of gene targeting was revolutionized through the application of sequence specific recombinases as tools for genomic engineering. A number of bacterial and yeast recombinase enzymes are able to rearrange DNA at specific target sequences. Gene modification employing site specific recombinases was pioneered using the Cre/*loxP* recombination technology (Rajewsky et al., 1996). The site specific DNA recombinase Cre (causes recombination) of the bacteriophage P1 recognizes specifically 34 bp long sequences, called *loxP* (locus of X over in PI) (Sternberg, 1981, Sternberg and Hamilton, 1981). Cre-mediated catalysis results in a reciprocal recombination between the two similarly oriented *loxP* sites and the consequent excision of the DNA segment between the *loxP* sites leaving behind a single *loxP* site (Sauer and Henderson, 1988). In the conditional allele, an essential region (typically a critical exon) of a gene of interest is flanked by two directly repeated *loxP* sites (floxed) positioned in non-coding regions. In this study we used a mouse line with *loxP* site flanking the exon 8-9 of *Smad4* allele. After the catalysis of recombinase, these two exons are excised and as consequence there is the lost of *Smad4* functional expression. To investigate the effect of deletion of *Smad4* in adult mice we used an inducible Cre recombinase, $CreER^{T2}$, actives only in presence of the estrogen modified Tamoxifen. Moreover the transgenic lines used have the $CreER^{T2}$ under the control of smooth muscle myosin heavy chain promoter, specific for the smooth muscular tissues.

Inducible expression system used to modulation of TGF-β/BMP signaling in VSMCs of adult mice

The regulation of transgene expression in transgenic mouse line may be an important tool to improve the specificity and quality of data obtained, especially if the aim is to study the effects in adult animal. Using KO mice or

common transgenic lines, we observe, in the adult animal, phenotypes that could be consequence of altered development and behavior of different cell types, and not directly associated to lack or to overexpression of the gene implicated.

To help in getting over this possibility, in the last few years most laboratories had used an inducible expression system named the Tet-On system. This system comprises two principal elements: a reverse tetracycline transactivator (rtTA) and a Tetracycline Responsive Element (TRE) prior to a CMV minimal promoter. The sequence of rtTA derived from a modified bacterial TetRepressor, linked to a VP16 domain, which is capable to bind a Tetracycline Responsive Element. In the Tet-On system the rtTA binds the TRE and activates the expression from CMV promoter only after the binding with doxycycline molecules.

In this project we used an inducible expression system, to control the expression of different cDNAs implicated in TGF-βs signaling only in smooth muscular tissues. For this purpose we modified a specific BAC clone with homologous recombination, to insert sequence of rtTA at the coding region of *Smmhc* gene. The construct was then used to generate driver transgenic line, expressing rtTA only in smooth muscle cells. The cross of driver transgenic line with transgenic lines for responsive construct, permits to obtain mice in which modulate TGF-β and BMP signaling in VSMCs. This tool may permit to understand the role of TGF-β and BMP signaling in the appearance of aortic aneurysm, through activation or inhibition of two pathways in wt and *Fbn1* mutant background. Another advantage of this inducible system is the reversibility, that allows turning off the induction of target genes interrupting doxycycline treatment.